View metadata, citation and similar papers at core.ac.uk

brought to you by CORE

provided by Repositorio da Producao Cientifica e Intelectual da Unicamp


UNIVERSIDADE ESTADUAL DE CAMPINAS

Instituto de Física Gleb Wataghin

Daniel Antonio López Delgado

# Threshold theorem for a quantum memory in a correlated environment

Teorema do limiar para uma memória quântica em um ambiente correlacionado

CAMPINAS 2016

Daniel Antonio López Delgado

# Threshold theorem for a quantum memory in a correlated environment

## Teorema do limiar para uma memória quântica em um ambiente correlacionado

*Thesis presented to the Gleb Wagathin Institute of Physics of the University of Campinas in partial fulfillment of the requirements for the degree of Doctor in Sciences*

*Tese apresentada ao Instituto de Física Gleb Wataghin da Universidade Estadual de Campinas como parte dos requisitos exigidos para a obtenção do título de Doutor em Ciências*

Advisor/Orientador: Amir Ordacgi Caldeira

Co-advisor/Coorientador: Eduardo Peres Novais de Sá

ESTE EXEMPLAR CORRESPONDE À VERSÃO FINAL DA TESE DEFENDIDA PELO ALUNO DANIEL ANTONIO LÓPEZ DELGADO E ORIENTADA PELO PROF. DR. AMIR ORDACGI CALDEIRA

Campinas 2016

**Agência(s) de fomento e nº(s) de processo(s):** CNPq, 148763/2012-0

Ficha catalográfica
Universidade Estadual de Campinas
Biblioteca do Instituto de Física Gleb Wataghin
Lucimeire de Oliveira Silva da Rocha - CRB 8/9174

L881t

López Delgado, Daniel Antonio, 1987-
Threshold theorem for a quantum memory in a correlated environment / Daniel Antonio López Delgado. – Campinas, SP : [s.n.], 2016.

Orientador: Amir Ordacgi Caldeira.
Coorientador: Eduardo Peres Novais de Sá.
Tese (doutorado) – Universidade Estadual de Campinas, Instituto de Física Gleb Wataghin.

1. Memória quântica. 2. Correção quântica de erros. 3. Sistemas quânticos abertos. 4. Teorema do Limiar. I. Caldeira, Amir Ordacgi,1950-. II. Sá, Eduardo Peres Novais de,1972-. III. Universidade Estadual de Campinas. Instituto de Física Gleb Wataghin. IV. Título.

Informações para Biblioteca Digital

**Título em outro idioma:** Teorema do limiar para uma memória quântica em um ambiente correlacionado
**Palavras-chave em inglês:**
Quantum memory
Quantum error correction
Open quantum systems
Threshold theorem
**Área de concentração:** Física
**Titulação:** Doutor em Ciências
**Banca examinadora:**
Amir Ordacgi Caldeira [Orientador]
José Antonio Roversi
Marcus Vinícius Segantini Bonança
Frederico Borges de Brito
Gustavo Garcia Rigolin
**Data de defesa:** 15-12-2016
**Programa de Pós-Graduação:** Física

MEMBROS DA COMISSÃO JULGADORA DA TESE DE DOUTORADO DE **DANIEL ANTONIO LÓPEZ DELGADO – RA: 142418** APRESENTADA E APROVADA AO INSTITUTO DE FÍSICA “GLEB WATAGHIN”, DA UNIVERSIDADE ESTADUAL DE CAMPINAS, EM 15/12/2016.

**COMISSÃO JULGADORA:**

- Prof. Dr. Amir Ordacgi Caldeira
- Prof. Dr. José Antonio Roversi
- Prof. Dr. Marcus Vinícius Segantini Bonança
- Prof. Dr. Frederico Borges de Brito
- Prof. Dr. Gustavo Garcia Rigolin

A Ata de Defesa, assinada pelos membros da Comissão Examinadora, consta no processo de vida acadêmica do aluno.

**CAMPINAS**
**2016**

Para Paula, pelo amor e a paciência

# Acknowledgements

This work would not have been possible without the help and support of many people. I should start thanking my family for all the support they have given me through all these years. They are with me even if we are separated by half a continent. Paula is the family I chose, she has suffered and joyed with me through the finishing of this thesis. My friends past and present have been crucial both in the academic context and in sharing woes, happiness, physics and music.

My advisor, Amir, was patient and kind enough to let me find my own path while supporting me in every step of the way. My co-advisor, Eduardo, was fundamental to the development of the main part of the work presented here. To both of them, my sincere gratitude.

I thank CNPq for financial support during my four years as a doctoral student, and I hope the best for Brazilian science and education.

## Resumo

A criação de um computador quântico é um projeto que guia, ao mesmo tempo, avanços tecnológicos e um melhor entendimento das propriedades de sistemas quânticos e da Mecânica Quântica em geral. O teorema do limiar é derivado da teoria quântica de correção de erros e garante que, se o ruido estocástico que e afeta os componentes de um computador quântico encontra-se abaixo de um valor limite, podemos operar esse computador quântico confiavelmente. Investigamos como esse teorema é modificado quando consideramos uma memória quântica (a qual usa o código de superfície para corrigir erros) acoplada a um ambiente correlacionado. O limiar de erros nesse caso é relacionado à transição de fase ordem-desordem de um sistema de spin equivalente.



## Abstract

The design of a quantum computer is a project which drives, at the same time, technological advancement and a better understanding of the properties of quantum systems and of Quantum Mechanics in general. The threshold theorem comes from quantum error correction theory and it guarantees that, if stochastic noise affecting the components of a quantum computer is below some threshold value, we can operate this quantum computer reliably. We investigate how this theorem is modified when we consider a quantum memory (which uses the surface code to correct errors) coupled to a correlated environment. The error threshold in this case is related the order-disorder phase transition of an equivalent spin system.

# Contents

# Chapter 1

# Introduction

Quantum Information is currently in the cutting edge of physics research. It is a paradigm change, focusing the discussion of all physical processes and characteristics from the point of view of information. This information might be exchanged between systems or be related to their states. Quantum Information's point of view has already permeated and enriched several other branches of Physics, from Statistical Mechanics [1] to black holes research [2] and its advance has undoubtedly helped us understand more deeply and thoroughly Quantum Theory.

One of the most challenging and interesting concepts in Quantum Information is the idea of a *quantum computer*. This is a device implemented by a quantum mechanical system, in contrast to a conventional or "classical" computer which is implemented by a system that follows traditional boolean logic.

A *universal* quantum computer could possibly solve any computational problem and in that aspect it is analogous to a Turing machine (classical computer). The difference between them lies in the fact that some problems which are believed to be NP-complete (i.e. hard, prohibitively time-consuming) for classical computers are believed to be solved efficiently (i.e. in relatively short times) by quantum computers, due to features of Quantum Mechanics like entanglement and superposition [3].

As an example, the problem of simulating quantum systems is one of those that can not be solved efficiently using a classical computer. It actually was one of the original motivations for developing quantum computers [4].

The realization of a universal quantum computer would have important consequences for the way we do things like cryptography, which now-a-days relies on the difficulty of factoring large numbers (these numbers constitute the cryptographic keys with which we codify infor-

mation). On one hand, a quantum computer would be capable of factoring large numbers in short times thereby being capable of breaking encryption as we do it today. But, on the other hand, quantum cryptography enables cryptographic protocols that are unbreakable in principle [3].

There are a lot of different experimental candidates for a scalable architecture for a quantum computer. Some of those implementations involve superconducting devices [5], trapped ions [6], magnetic resonance [7], and optical phenomena [8], just to name a few. Some candidates do not follow the architecture of a universal quantum computer, like D-Wave's quantum annealer[1] [9, 10]. Albeit some of the experimental difficulties are daunting, the quantum information community is very positive about the prospect of constructing quantum computers in the mid-term.

In spite of this climate of optimism, there are fundamental questions to be answered. One of them has to do with the fact that quantum systems are very fragile, quantum coherence can be destroyed very quickly due to the system's interaction with its surroundings. So, how can we implement and protect a system such that we can store quantum information and compute reliably with it?

A related question is the one of scalability. Up to now only small devices (with a handful of few qubits), have been constructed. Thus, the physics of decoherence (loosely called quantum noise) in a large device, with thousands or millions of qubits is an open questions. Hence, we are bound to ask what are the limits for computation, or for storing information, within such a large device?

These questions are partially answered by the threshold theorem from fault tolerance theory. This theorem states that when the noise to which a quantum computer is subjected is below some threshold, the use of quantum error correction and fault tolerance procedures provides enough protection against the noise to allow for the computation to be very likely to succeed [3, 11].

The threshold theorem was introduced assuming stochastic error models. These models are customarily used to study decoherence in quantum information, in part because they are easier to manipulate and obtain results. But stochastic error models are not adequate for a large number of systems of interest, e.g. solid state ones [12].

[1] An annealer is basically a computer which solves the specific task of finding the minimum of some function. Although this may not seem interesting at first sight, it so happens that a lot of important and difficult problems can be mapped to the problem of finding the minimum of some function.

We are going to study the threshold theorem but using a Hamiltonian error model. We take a phenomenological approach that let us not worry about the details of the quantum computer's environment while still obtaining meaningful results. We only assume that the perturbation will be weak enough so that we can model it as a bath of harmonic oscillators which is analogous to approaches dealing with Brownian motion [13]. The advantage of our model is that it is more generic than an stochastic error model, and more adequate because it takes into account memory effects as well as temporal and spatial correlations between qubits [14].

Following [15, 16, 17], we investigate the time evolution of a quantum memory which uses a quantum error correction scheme known as the surface code. This problem is cast into an statistical mechanical language and the error threshold is then related to the critical parameters of an equivalent spin model.

In the following Chapters we review the basic concepts which we use throughout the text, but we are aware that no text can be completely self-contained. Some notions of quantum and statistical mechanics are assumed. In addition, some knowledge about many-body physics and of open quantum systems would facilitate the reading but is not indispensable. We will introduce the concepts of quantum information that we need for our work, but for a better understanding on then we recommend Nielsen and Chuang's book [3]. Although this book does not encompass the latest developments in the field of Quantum Information, it constitutes a very comprehensive guide to its basic concepts.

The structure of this work is as follows:

- In Chapter 2 we start by introducing the fundamental concepts of Quantum Information that we use throughout the text. We also explain here how quantum error correction works, the details of the surface code and the original version of the threshold theorem.

- Chapter 3 deals with open quantum systems' theory: we review the system-plus-environment approach, the famous Markovian approximation and stochastic models. Here we revisit the threshold theorem to show how it is modified by the presence of a correlated environment.

- Chapter 4 contains our original results. Here we study the evolution of a quantum memory coupled to a correlated environment via surface code and drive the equivalent of our error threshold for this situation.

- Chapter 5 has our final remarks and the possible directions in which our work can be extended.

- We left some details of the calculations to Appendixes A and B.

# Chapter 2

# Quantum error correction

**Quantum Error Correction Sonnet**

We cannot clone, perforce; instead, we split
Coherence to protect it from that wrong
That would destroy our valued quantum bit
And make our computation take too long.

Correct a flip and phase - that will suffice.
If in our code another error's bred,
We simply measure it, then God plays dice,
Collapsing it to X or Y or Zed.

We start with noisy seven, nine, or five
And end with perfect one. To better spot
Those flaws we must avoid, we first must strive
To find which ones commute and which do not.

With group and eigenstate, we've learned to fix
Your quantum errors with our quantum tricks.

Daniel Gottesman

We established in the introduction that quantum information, and in particular quantum computers, are compelling as a research topic and as a technology. But, as we also remarked, environmental noise constitutes a fundamental obstacle that must be addressed. Thus the application of quantum error correction methods is indispensable.

As its name implies, quantum error correction deals with correcting errors in the information stored in and manipulated by quantum computers. This is essential since these systems are very fragile, and thus information codified in them is prone to errors due to the quantum computer's interaction with its surroundings (also referred to as environment).

We leave for Chapter 3 the details of this system-environment interaction. Right now we are going to describe the nature of the quantum information we want to store and how we can protect it from damage.

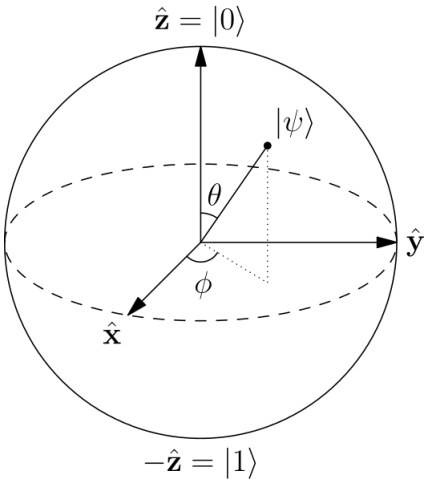


Figure 2.1: Bloch sphere. Glosser.ca "Bloch Sphere" August, 2016, via Wikimedia, Creative Commons Attribution.

The basic unit of information for classical computers is the bit. A bit can take values $0$ or $1$. On the other hand, the basic unit of quantum information is the qubit, the difference with its classical counterpart is that it can not only take values $0$ or $1$, but it can be in an state which is a superposition of those basic states.

A qubit is implemented by a two-level system. We label its states as $|0\rangle$, and $|1\rangle$, using Dirac's notation. As we said, a qubit can be in any of its reference states or in a superposition of them, in general we can write its state as:

$$|\psi\rangle = \alpha|0\rangle + \beta|1\rangle. \tag{2.1}$$

The possible states of a qubit can be represented by the surface of a sphere called the Bloch sphere (Figure 2.1) by making the parametrization $\alpha = \cos\frac{\theta}{2}$ and $\beta = e^{i\phi}\sin\frac{\theta}{2}$. Then we can rewrite Equation (2.1) as:

$$|\psi\rangle = \cos\frac{\theta}{2}|0\rangle + e^{i\phi}\sin\frac{\theta}{2}|1\rangle. \tag{2.2}$$

This geometrical representation of a qubit is useful for our discussion since it becomes evident how an error in a classical bit is different from one in a qubit. Classical bits are only affected by errors which flip their value (take a $0$ to $1$ or vice versa), called *bit flips*. But qubits can have their state continuously changed by a certain error, thus quantum information needs to be protected from bit flips, phase flips, and their continuous linear superpositions.

Although it seems we would need to protect the quantum information from a potentially

infinite number of errors, in Section 2.1.2 we show how we actually only need to account for a finite set of them in order to perform quantum error correction successfully. An example of this is that by protecting the qubit from bit flips and phase flips, we are automatically protecting it against linear combinations of those two kind of errors.

Here we are interested in quantum memories. Those memories are composed by a collection of qubits such that we can store some quantum information as their state. We want to determine under what conditions we can prepare a system (a quantum memory) in a particular state and be sure that after an arbitrary time this state will remain unperturbed.

There exist two different strategies to protect the quantum information that we store in a quantum memory. These are the passive and active approaches. Passive approaches involve designing a system which, due to its internal dynamics, remains in the state in which we initialized it. Active approaches involve codifying the quantum information in a system which we measure periodically. This measurements are such that they do not give us any details of the information we stored but they will show us what errors have appeared in this information so that we can correct them.

At first glance, passive quantum memories seem like the obvious choice. Why would we want the overhead of measuring our system just to check for errors? Well, simply because constructing such passive memories has proven a formidable task [18, 19]. And even using the best passive correction schemes, we should use active correction to make sure there is no residual decoherence that would damage the information we stored.

For more information on the topic of passive quantum memories we leave here some references: the canonical example for passive quantum memories is Kitaev's toric code [20], a review of current research in that field was done by Brown et. al. [18], and possible implementations using superconducting qubits were reviewed by Douçot and Ioffe [19].

From now on, we concentrate on the study of *quantum error correction* methods. As done in the literature, the word "active" is implied here. In the next Sections we do not leave out important formal results, but we try to approach the topic as intuitively as possible.

## 2.1 Quantum error correction theory

If we were to synthesize last Section, we could say that quantum error correction is a method used to protect quantum information from the decoherence resulting of the interaction of the

quantum system with its environment. In this Section we investigate exactly how quantum error correction is performed. We are going to follow mainly references [3] and [11].

Each error correction scheme is called a code because it codifies the information in a clever way, mainly by adding redundancy. This makes the information less susceptible to errors.

Let us start by explaining how a simple classical error correction code works before going to the quantum case. This will help us show the basics of error correction as plainly as possible.

The more straightforward classical error correction code is the repetition code. Basically, the idea with this code is to protect the information by copying it a number of times. We could say that an analogy to this protocol is repeating what you say in a noisy phone call, so you interlocutor can understand what you are saying.

To implement this protocol, we start from an information bit $s$, which can take the values $0$ or $1$. Say we want to store this bit for some time and being able to read its state later[1]. During this time, there is a probability $\epsilon$ of the bit changing its state (from $0$ to $1$ or the contrary). Notice that this implies that $1-\epsilon$ is the probability of the bit maintaining its original state.

To keep things as simple as possible, we use here the smallest repetition code: the three-bit repetition code. Then we require only two copies of our bit $s$. The original bit and each of its copies are called physical bits and the whole of them is the logical bit $\bar{s}$. Finally, since the original bit can take the values $0$ or $1$, we have:

$$s = 0 \quad \rightarrow \quad \bar{s} = 000 \tag{2.3}$$

$$s = 1 \quad \rightarrow \quad \bar{s} = 111. \tag{2.4}$$

But why is this beneficial? To answer this, we need to compare the probability $\epsilon$ of the original bit to get corrupted with the corresponding probability $\bar{\epsilon}$ for the logical qubit. To this end we assume that the probabilities of errors in each bit are independent.

We also need to clarify now the complete error correction procedure with the repetition code:

- encoding: we encode the original bit by making copies of it,
- storage: we store our logical bit for later use, and

[1] Normally these ideas are presented in terms of transmitting information, but since our focus is in quantum memories the concept of storage of the information is more adequate.

| Logical bit state $\bar{s}$ | 110 | 010 | 111 |
|---|---|---|---|
| Decoded state $s$ | 1 | 0 | 1 |

Table 2.1: Decoding step.

- decoding (majority vote): the final state of the bit will be determined by the state of the majority of the physical bits, see Table 2.1.

Then, given an initial logical bit, e.g. $\bar{s} = 000$, only one of the physical bits can have an error (bit flip) during storage so that the logical bit is not corrupted (i.e. $s = 0$ will be the state after decoding). Otherwise the information is altered at the end of the procedure. Following our example, we would get $s = 1$ after decoding if two or three of the physical bits flipped their state.

Then there are four different final configurations in which the bit's information is not damaged: $000$, $001$, $010$, and $100$. While $000$ has probability $(1-\epsilon)^3$ to be the final state, each of the other three states have probability $(1-\epsilon)^2\epsilon$ to be so. Then, the probability $p$ of the logical

$$p = (1-\epsilon)^3 + 3(1-\epsilon)^2\epsilon = 1 - 3\epsilon^2 + 2\epsilon^3, \tag{2.5}$$

and the probability of the logical bit's original state be corrupted is

$$\bar{\epsilon} = 1 - p = 3\epsilon^2 - 2\epsilon^3. \tag{2.6}$$

Notice that this expression involves terms to the power of $2$ and $3$, then for small error rates $\epsilon$ we expect $\bar{\epsilon}$ to be even smaller. Let us check if that holds true:

$$\bar{\epsilon} < \epsilon \implies 3\epsilon^2 - 2\epsilon^3 < \epsilon \implies 0 < 2\epsilon^2 - 3\epsilon + 1. \tag{2.7}$$

This inequality is met by values $\epsilon < 1/2$ or $\epsilon > 1$. And, since we are dealing with probabilities ($0 \leq \epsilon \leq 1$), we conclude that if $\epsilon < 1/2$, then $\bar{\epsilon} < \epsilon$. This means that, when the probability of errors for the physical bits is below $1/2$, codifying the original bit with the repetition code actually makes it less probable that we lose information.

Now we are going to study error correction for the quantum regime. The fundamental unit of quantum information is the qubit: it is realized by a two-state system in which each of its states correspond to the classical states, i.e. $1 \to |1\rangle$, and $0 \to |0\rangle$. But, since now we are

in the quantum regime, the qubit can not only be prepared in any of its two states, as it can also be in a superposition of its states, as we wrote in Equation (2.1).

As a first approach we would like to see if classical codes could be used for quantum information: can we apply the repetition code in the quantum case? The answer is no, because it is impossible to make copies of an arbitrary quantum state through unitary transformations. This result is known as the *no-cloning theorem* [3, 21] and it can be understood very simply, by contradiction.

Imagine that it exists a unitary operation $U$ which can make copies of arbitrary quantum states, e.g. $|\psi\rangle$ and $|\phi\rangle$. Then it follows that:

$$U\left(|\psi\rangle|s\rangle\right) = |\psi\rangle|\psi\rangle \tag{2.8}$$

and

$$U\left(|\phi\rangle|s\rangle\right) = |\phi\rangle|\phi\rangle. \tag{2.9}$$

The contradiction arises because these two equations imply that:

$$\langle\psi|\phi\rangle = |\langle\psi|\phi\rangle|^2,$$

which is only possible if $\langle\psi|\phi\rangle = 0$ or $\langle\psi|\phi\rangle = 1$, i.e. either $|\psi\rangle = |\phi\rangle$ or $|\psi\rangle$ is orthogonal to $|\phi\rangle$. Thus $|\psi\rangle$ and $|\phi\rangle$ cannot be arbitrary states.

Other difficulties we need to overcome in order to create quantum error correction codes are the fact that measurements in quantum mechanics destroy the quantum state being measured[2], and that errors are continuous (as we exemplified with the Bloch sphere, Figure 2.1).

Luckily for us, these aspects of quantum theory do not prevent us from being able to do quantum error correction. Although the repetition code can not be implemented with quantum systems, there is a very straightforward adaptation to it: it is the qubit bit-flip code. Again we are going to study the simplest case with three physical qubits, but the generalization to any number of physical qubits is straightforward.

Let us start by clarifying that although we can not copy the state of our qubit, by adding ancillary qubits and operating on them, we can create states such that, if $|s\rangle = |0\rangle$ then

[2]When we measure the qubit $|s\rangle$ on the basis of its states what we get is $|0\rangle$ with probability $|\alpha|^2$ or $|1\rangle$ with probability $|\beta|^2$.

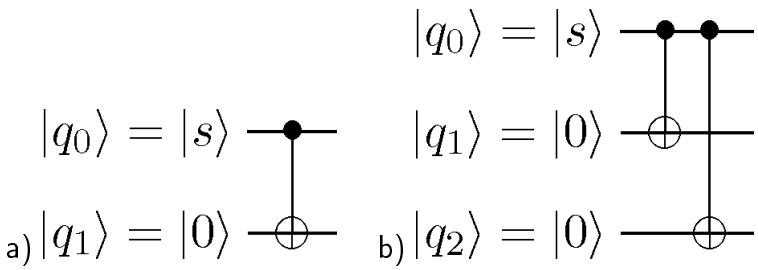


Figure 2.2: a) CNOT gate. b) Quantum circuit for the three qubit bit flip code.

$|\bar{s}\rangle = |000\rangle$, and if $|s\rangle = |1\rangle$ we have $|\bar{s}\rangle = |111\rangle$[3]. Moreover, we can encode the state of our qubit (Equation (2.1)) as:

$$|s\rangle = \alpha|0\rangle + \beta|1\rangle \rightarrow |\bar{s}\rangle = \alpha|000\rangle + \beta|111\rangle. \tag{2.10}$$

As we will see, this encoding results in a similar gain as we had for the classical case with the repetition code. But before we enter in the details of why this is so, we will explain how we can create the logical qubit $|\bar{s}\rangle$ in Equation (2.10).

The encoding process is done through unitary operations known as gates. Gates can be expressed as matrices, and can operate on just one or various qubits at a time.

Here we will use the controlled-NOT or CNOT gate. This gate involves applying a NOT gate to a qubit (known as target) depending on the state of another qubit (known as control). A NOT gate involves only one qubit, it simply applies a $\sigma^x$ Pauli operator to the state of a qubit, i.e. $|0\rangle \overset{\text{NOT}}{\longleftrightarrow} |1\rangle$.

A CNOT gate is such that when the control qubit is in the $|0\rangle$ state, it leaves the target qubit untouched. On the other hand, if the state of the control qubit is $|1\rangle$, then a NOT gate is applied to the target qubit. Figure (2.2-a) shows the representation of a CNOT gate where the control qubit is $|q_0\rangle$ in the state $|s\rangle$, and the target qubit is $|q_1\rangle$ in the state $|0\rangle$. The action of the CNOT gate for the case where $|s\rangle$ is given by Equation (2.2) is:

$$|s\rangle|0\rangle = \alpha|0\rangle|0\rangle + \beta|1\rangle|0\rangle \overset{\text{CNOT}_{01}}{\longrightarrow} \alpha|0\rangle|0\rangle + \beta|1\rangle|1\rangle = \alpha|00\rangle + \beta|11\rangle. \tag{2.11}$$

It is straightforward now to understand that the quantum circuit[4] in Figure (2.10-b) takes the state $|s\rangle$ (given again by Equation (2.2)), and encodes it as we stated in Equation (2.10).

As in the classical case we want to determine if this encoding is beneficial for our purposes.

[3] Here $|000\rangle = |0\rangle|0\rangle|0\rangle = |0\rangle \otimes |0\rangle \otimes |0\rangle$, and similarly for $|111\rangle$.

[4] A quantum circuit is a graphic representation of operations done on a number of qubits. Each qubit is represented by an horizontal line, and time runs to the right.

To that end we review the error correction process again, adapting it to the specificities of the quantum case:

- encoding: use ancillary qubits to encode our original qubit,
- storage: we leave our qubit for posterior use,
- error detection or syndrome extraction: we measure our qubit using an specific set of projection operators so that we obtain information about the errors that happened to our qubit, but we do not have information about its actual state.
- recovery: once we know what error happened to the physical qubits, we can apply the appropriate operations ($\sigma^x$ operators) to recover the original state. This is simply done by flipping back the faulty physical qubit.

The syndrome extraction is an essential part of the process and it is different to the decoding we performed in the classical case. Thus we need to expand on it now.

The projection operators we mentioned are:

$$\begin{cases} P_0 &= |000\rangle\langle 000| + |111\rangle\langle 111| \\ P_1 &= |100\rangle\langle 100| + |011\rangle\langle 011| \\ P_2 &= |010\rangle\langle 010| + |101\rangle\langle 101| \\ P_3 &= |001\rangle\langle 001| + |110\rangle\langle 110| \end{cases} \tag{2.12}$$

During syndrome extraction, one of these operators will return a value $1$, and the others $0$. If we measure the evolved state $|s'\rangle$ of the qubit after storage, using the projection operators, and obtain: $\langle s'|P_0|s'\rangle = 1$, and $\langle s'|P_i|s'\rangle = 0$ for $i = 1, 2, 3$, then we know that no errors occurred. On the other hand, when $P_1$ ($P_2$ or $P_3$) is the projector that has value one when measured, we know that there was an error (bit flip) on the first (second or third) physical qubit.

Notice that the state of the qubit is unaltered by the measurement of these projection operators. This is because for a given arbitrary state $|s\rangle$ we either have $P_i|s\rangle = |s\rangle$ or $P_i|s\rangle = 0$ ($i \in \{0, 1, 2, 3\}$).

In analogy with the classical case, problems arise though if two physical qubits are flipped. Suppose we start with a $|000\rangle$ logical qubit. If bit flips occurred to two of the physical qubits during storage, we get any of the final states $|011\rangle$, $|101\rangle$ or $|110\rangle$. The projection operator's

measurement leads us to interpret the final state as $|111\rangle$, with one physical qubit flipped. The recovery operation would then fail: it would flip the remaining qubit and make $|111\rangle$ be the final state.

Since this situation is analogous to the classical case, the calculus of the probability of success and failure is the same. Assuming the probability of a bit flip $\epsilon$ is independent for each of the physical qubits, the probability of successfully correct an error will be given by Equation (2.5), the probability of failing is given by Equation (2.6), and using this error correcting code is advantageous when $\epsilon < 1/2$.

This discussion also help us to identify one of the oversimplifications on several approaches to quantum error correction. As beautifully presented by Richard Feynman in his famous book "the Feynman's Lectures", if there are two possible quantum paths in an evolution that could not be distinguished, then the system takes both paths. In the three qubit code initially prepared in the state $|000\rangle$, then after evolving for a time $t$ and a syndrome $P_0$ is found, it means that the normalized quantum state is $|000\rangle + A|111\rangle$, where $A$ is an amplitude that can be related to $p$. Hence, the limits to the protection that a code can offer to a system is the amplitude of a logical error after an evolution. This subtlety is some times overlooked, but it is in the core of the threshold for the surface code that we will discuss.

### 2.1.1 General framework for quantum error correction

We made some progress towards understanding quantum error correcting codes with the bit flip error code: we saw how to bypass the no-cloning theorem and how to measure the qubits for errors without damaging the information they contain. But there is still one obstacle that we mentioned before: the set of errors that can affect quantum information is far greater than the one affecting classical information.

To see how to overcome this difficulty, we need to understand what kinds of errors can be dealt with in general using a quantum error correcting code. In the following lines we follow mainly [22], but we also take some ideas from [3].

Let us start with some notation. We call $C$ the code space: this is a Hilbert space composed by the set of logical states, it is also a sub-space of a larger Hilbert space. Logical states are the ones we use to encode the information. They are also called *codewords*, e.g. $|000\rangle$ and $|111\rangle$ are the three-qubit code's codewords.

We denote $\mathcal{E}$ as the set of possible errors. This errors take the form of tensor products of

operators:

$$E_a = \bigotimes_i O_{i,a}, \tag{2.13}$$

where $a$ labels different errors and $i$ labels the qubits. For example, errors in the three-qubit code were bit flips, i.e. $\sigma^x$ Pauli operators acting on any of the physical bits. Then, for this example: $O_i \in \{\sigma_i^x\}$, $i = 1, 2, 3$.

Not all errors can be detected and corrected by the code. The set of *correctable errors* is denoted $\mathcal{E}_c$. If $E_a \in \mathcal{E}$ but $E_a \notin \mathcal{E}_c$, then $E_a$ is an *uncorrectable error*.

How do we notice that an error happened? When correctable errors occur, syndrome extraction leads to the state of the qubit being projected onto a sub-space perpendicular to $C$. But when an uncorrectable error occurs the state of the qubit remains in $C$, thus the error goes unnoticed.

We can exemplify this with the three-qubit code and in Figure 2.3 we show a visual representation of correctable and uncorrectable errors related to this code. In the figure, $C$ is the plane defined by vectors $|000\rangle$ and $|111\rangle$.

When a correctable error occurs, syndrome extraction projects the faulty state onto a plane perpendicular to $C$. This plane corresponds to either of the sub-spaces defined by $P_1$, $P_2$ or $P_3$ (Equation (2.12)), depending on the particular error.

On the other hand, an uncorrectable error will keep the state of the system in $C$, i.e. the faulty state remains in the plane defined by the codewords.

Now we will put this into equations. We label two different codewords $|i\rangle$ and $|j\rangle \in C$. For correctable errors to be perfectly distinguishable, they have to take the codewords to orthogonal states, as we just discussed, i.e.:

$$\langle i|E_a^\dagger E_b|j\rangle = 0, \tag{2.14}$$

for $E_a$, $E_b \in \mathcal{E}_c$.

Moreover, correctable errors need to be such that:

$$\langle i|E_a^\dagger E_b|i\rangle = C_{ab}. \tag{2.15}$$

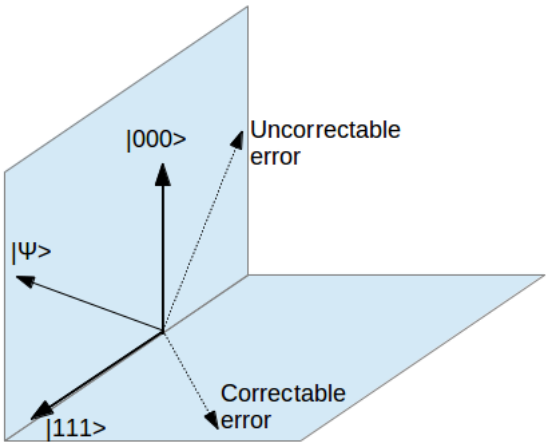


Figure 2.3: Visualization of correctable and uncorrectable errors for the three-qubit code. $|000\rangle$ and $|111\rangle$ are the codewords, and $|\Psi\rangle$ is the original state of the qubit. Correctable errors can be detected because, when they occur, syndrome extraction projects the state of the qubit onto a sub-space which is orthogonal to the code space. Uncorrectable errors maintain the state of the qubit in the code space, thus being undetectable.

Also, notice that the last condition implies that

$$\left(\langle i|E_a^\dagger E_b|i\rangle\right)^\dagger = C_{ab}^* \tag{2.16}$$

and

$$\left(\langle i|E_a^\dagger E_b|i\rangle\right)^\dagger = \langle i|E_b^\dagger E_a|i\rangle = C_{ba}. \tag{2.17}$$

Thus $C_{ab}$ ~~is~~ has to be a Hermitian ($C_{ba} = C_{ab}^*$) matrix and it does not depend on the state $|i\rangle$. This condition has to be met because otherwise we would get information about the encoded state, and thus we would destroy it by doing syndrome extraction.

These two conditions can be summarized as:

$$\langle i|E_a^\dagger E_b|j\rangle = C_{ab}\delta_{ij} \tag{2.18}$$

Another way this is written in the literature is by using the projectors $P$ onto $C$: $P = \sum_i |i\rangle\langle i|$, for $|i\rangle \in C$. Then the error correction condition is:

$$PE_a^\dagger E_b P = C_{ab}P, \tag{2.19}$$

which clearly is equivalent to Equation (2.18). This is the form which is used in [3].

### 2.1.2 Discretization of errors

In this Section we show that we only need to design an error code that accounts for a finite number of errors to get protection against an infinite number of arbitrary errors.

In particular, we are going to show that errors which are linear combinations of elements of $\mathcal{E}_c$ are also correctable errors. I.e., if

$$F_j = \sum_i m_{ij} E_i, \tag{2.20}$$

where the $m_{ij}$ is a matrix of complex numbers and $E_i \in \mathcal{E}_c$, then $F_j \in \mathcal{E}_c$.

To prove this, we start from Equation (2.18), which characterizes correctable errors. Without loosing generality, we will assume that $C_{ab}$ is diagonal, i.e. $C_{ab} = C_{aa}\delta_{ab}$.

We are going to see how this condition behaves when we use errors that are linear combinations of $E_i$, as in Equation (2.20). To that end we substitute $E \to F$ on the left hand side of Equation (2.18), and writing to $F_j^\dagger = \sum_i m_{ij}^* E_i^\dagger$ we get:

$$\begin{aligned}\langle i|F_a^\dagger F_b|j\rangle &= \langle i|\sum_{a'} m_{a'a}^* E_{a'}^\dagger \sum_{b'} m_{b'b} E_{b'}|j\rangle = \sum_{a'b'} m_{a'a}^* m_{b'b} C_{a'b'}\delta_{a'b'}\delta_{ij} \\ &= \sum_{a'} m_{a'a}^* C_{a'a'} m_{a'b}\delta_{ij} = \bar{C}_{ab}\delta_{ij}.\end{aligned} \tag{2.21}$$

Now we need to determine whether $\bar{C}_{ab} = \sum_{a'} m_{a'a}^* C_{a'a'} m_{a'b}$ is Hermitian or not. If it is, the error correction criteria holds for the errors $F$, which is what we want to prove.

$\bar{C}_{ab}$ is Hermitian, if $\bar{C}^\dagger = \bar{C}$, i.e. $\bar{C}_{ba}^* = \bar{C}_{ab}$. Let us see:

$$\bar{C}_{ba}^* = \left(\sum_{a'} m_{a'b}^* C_{a'a'}^* m_{a'a}\right)^* = \sum_{a'} m_{a'b} C_{a'a'}^* m_{a'a}^*. \tag{2.22}$$

And, from the fact that $C_{ab}$ is Hermitian, we conclude that $\bar{C}_{ab}$ is Hermitian too.

## 2.2 Threshold theorem

Under what conditions can we scale a quantum computer and operate it for an extended time without errors propagating and corrupting the information? This is the question answered by the threshold theorem and studied under the concept of fault tolerant quantum computation. This theorem will be the focus of this thesis.

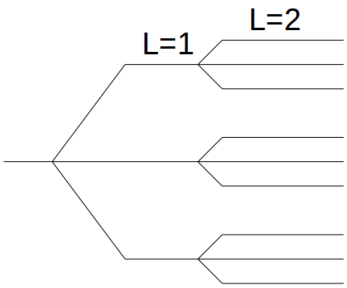


Figure 2.4: Concatenation of three qubit code.

Here we will present the threshold theorem in the framework of stochastic error models: in this Section we assume that errors are aleatory and independent. We devote Sections 2.4.1 and 4.2.1 and Chapter 4 to expand this theorem further and show how it is applied to other types of error models.

Under this assumption (aleatory and independent errors), the *threshold theorem* guarantees that if the error probability affecting individual quantum gates $\epsilon$ is below some threshold (the *accuracy threshold* $\epsilon_{\text{th}}$), then we can perform arbitrarily long quantum computations.

The key to this theorem is the concept of concatenation. It consists in encoding the information various times over: imagine we use an error correction code once from physical qubits, that would be level $1$ concatenation. We would need $n$ physical qubits, $n$ depending on the specific code. Level $2$ concatenation then requires us to take the resulting logical qubits from level $1$ concatenation and using them as building blocks for another implementation of the same error correction code. Notice that now we would need $n^2$ physical quibits.

Then $L$ levels of concatenation require $n^L$ physical qubits. For the three-qubit code, for example, $n = 3$. Figure 2.4 illustrates the first two concatenation levels for the three-qubit code.

We show now why concatenation is useful. Suppose there is a failure at the first level of encoding, $L = 1$. For the three-qubit code this implies that there were errors in at least two physical qubits. The probability of this happening being:

$$p_1 \approx c\epsilon^2 \approx \alpha^2\epsilon^2, \tag{2.23}$$

$\epsilon$ here is the error per qubit per appropriate unit of time (the time to perform quantum error correction or eventually implement a quantum gate), and $\alpha$ is the number of locations in the quantum circuit where an error can affect a single qubit before error correction.

At level of encoding $L = 2$, the failure probability is

$$p_2 \approx c p_1^2 \approx \alpha^2 \left(\alpha^2 \epsilon^2\right)^2 . \tag{2.24}$$

Then, for $L$ levels of encoding we have the general expression:

$$p_L \approx c p_{L-1}^2 \approx \frac{\left(\alpha^2 \epsilon\right)^{2^L}}{\alpha^2}. \tag{2.25}$$

Suppose our computation takes $T$ logical quantum gates to be performed, then we want to compute for a time $t = T\tau$, $\tau$ being the time it takes to perform each gate. To accomplish this computation with *accuracy* $\epsilon_{\text{th}}$, we need $L$ levels of concatenation such that:

$$p_L \approx \frac{\left(\alpha^2 \epsilon\right)^{2^L}}{\alpha^2} \leq \frac{\epsilon_{\text{th}}}{T}. \tag{2.26}$$

If the condition $\epsilon < \epsilon_{\text{th}} \equiv 1/\alpha^2$ is met, this inequality can be solved for $L$:

$$L > \bar{L} \approx \log \left[ \frac{\log \left(T/\alpha^2 \epsilon_{\text{th}}\right)}{\log \left(1/\alpha^2 \epsilon\right)} \right]. \tag{2.27}$$

Finally, the number of qubits required is $n_{tot} = n^{\bar{L}}$, thus:

$$n_{tot} = \left[ \frac{\log \left(T/\alpha^2 \epsilon_{\text{th}}\right)}{\log \left(1/\alpha^2 \epsilon\right)} \right]^{\log n}. \tag{2.28}$$

As we see $n_{tot}$ only grows polylogarithmically (and not exponentially) with $T$ and $1/\epsilon$, which means that it is feasible to implement concatenation experimentally.

The downside to the concatenation is obvious, although the number of physical qubits required does not grow exponentially with time, it does can become very large.

### 2.2.1 Error threshold as a phase transition

Dorit Aharonov's paper [23] is fundamental to introduce this approach. In that work, Aharonov studied a quantum computer constituted by $n$ qubits embedded in a $d$-dimensional lattices. She noticed that the behavior of the accuracy threshold for quantum error correction reminds one of a phase transition: there exist two regimes, one in which quantum computing is possible (when the local noise rate $\epsilon$ is below the error threshold $\epsilon_{\text{th}}$) and another in which the quantum computer can be simulated efficiently using a classical computer (local noise rate above $\epsilon_1 > \epsilon_{\text{th}}$).

To further this analogy, Aharonov investigates the entanglement shared by spatially separated parts of the system (quantum computer), when $n \to \infty$, using the concept of entanglement length. Entanglement length is the rate at which the entanglement between those parts of system decays with the distance between them. It is also analogous to the correlation length.

The interesting outcome of this analysis is that those two regimes related to the local noise are also characterized by two different behaviors of the entanglement length:

- below the error threshold, $0 \leq \epsilon < \epsilon_{\text{th}}$, the entanglement length is infinite, i.e. there is long range entanglement in the system;
- above a higher value for the rate of local noise, $\epsilon_1 < \epsilon \leq 1$, entanglement length is finite, so that entanglement decays exponentially with distance.

This results lead to the inference that there exists a phase transition in the system at a non-trivial local noise rate $\epsilon_c$, such that $\epsilon_{\text{th}} < \epsilon_c < \epsilon_1$, and the entanglement length can be used as an order parameter to characterize this phase transition.

## 2.3 Stabilizer codes

We now start to specialize on the specific type of error correcting code that we are going to study: the surface code. But since the surface code uses the stabilizer formalism as its basis, we start by presenting briefly this formalism. We follow mainly [3].

### 2.3.1 Stabilizer formalism

When working in the stabilizer formalism we do not focus on the state of the system, or the codewords for quantum error correction. Instead we work with a set of operators $\{S_i\}$, the *stabilizer operators*, which then define the set $V_S$ of possible states (or codewords) such that

$$S_i|\psi\rangle = |\psi\rangle. \tag{2.29}$$

Let us give here an example: we will specify the codewords of the three qubit bit-flip code using the stabilizer formalism. This can help us better understand the abstract constructions we will introduce later.

Say we have the stabilizer operators:

$$S_1 = \sigma^z \sigma^z I, \text{ and } S_2 = \sigma^z I \sigma^z. \tag{2.30}$$

Then we can find states $|\psi\rangle$ such that $S_1|\psi\rangle = |\psi\rangle$, and $S_2|\psi\rangle = |\psi\rangle$. For $S_1$ we have: $|000\rangle$, $|001\rangle$, $|110\rangle$, and $|111\rangle$. For $S_2$ we have: $|000\rangle$, $|010\rangle$, $|101\rangle$, and $|111\rangle$. Then the common states for $S_1$ and $S_2$ are $|\psi\rangle = |000\rangle$, and $|\psi\rangle = |111\rangle$, which coincide with the codewords of the three qubit code. We will come back to the three qubit code later on.

Now, in general, to construct the stabilizer operators for one qubit, we use the Pauli's group $G_1$[5] (the subindex just indicates that this is Pauli's group for one qubit). The elements of this group are the Pauli's matrices and the identity, and the group's operation is the matrix product. Explicitly the elements of $G_1$ are:

$$\{\pm I, \pm iI, \pm\sigma_x, \pm i\sigma_x, \pm\sigma_y, \pm i\sigma_y, \pm\sigma_z, \pm i\sigma_z\}, \tag{2.31}$$

where we include elements with $-1$, and $i$ factors to ensure that $G_1$ is in fact closed under the matrix product.

$G_n$ corresponds then to the Pauli's group for $n$ qubits and its elements are simply the tensor product of the elements of $G_1$ (e.g. $G_n$'s identity element is $I_1 \otimes I_2 \ldots \otimes I_n$).

Now we can define the so-called *stabilizer* $S$. The stabilizer is a subgroup of $G_n$ which specifies a set of states $V_s$. $V_s$ is formed by the common eigen-states of the elements of $S$. We say that $V_s$ is the vector space stabilized by $S$, or that $S$ is $V_s$'s stabilizer, because the elements from $V_s$ are stable (invariant) over the action of the elements in $S$.

Another important concept is the one of the group's *generators*. We actually implicitly used it in our example of the three qubit code. We saw that the set $S' = \{S_1, S_2\}$ (Equation (2.30)) specifies the codewords of the three qubit bit-flip code. But notice that the set $S = \{I, S_1, S_2, S_3\}$, with $S_3 = I\sigma^z\sigma^z$, would also work.

Here $S_1$ and $S_2$ are the generators of the group $S$. Notice that they *generate* the elements of this group, since $S_1 S_1 = I$, and $S_1 S_2 = S_3$. We will use the notation $S = \langle S_1, S_2 \rangle$ to denote the generators of group $S$.

As final remarks, notice that the elements in $S$ must all commute with each other so it

[5] An introduction to group's theory can be found in Arfken and Weber's book [24]. For us it is sufficient to specify that a group is a closed set of elements and an operation. Each of the elements needs to have an inverse, the operation has to be associative, and the identity element must exist.

exists a common set of states for them. Also $-I \notin S$, since $-I|\psi\rangle \neq |\psi\rangle$ unless $|\psi\rangle$ is a trivial (null) state.

### 2.3.2 Quantum error correction with stabilizer codes

Using the stabilizer formalism we can start defining error correcting codes: a stabilizer code $C(S)$ is defined by the vector space $V_S$ which is stabilized by the subgroup $S$ of $G_n$. We use the notation $[n, k]$ to characterize $C(S)$ meaning that it utilizes $n$ physical qubits, encodes $k$ logical qubits, and its subgroup $S$ has $l = n - k$ generators.

#### Error correction conditions for stabilizer codes

Now a natural question to ask is, what kind of errors can this code correct? In general terms, and as we saw in Section 2.1, error operators that take a state in $V_S$ to an orthogonal state (or linear combinations of them) are the ones that can be detected with certainty and corrected. Let us expand on this in the following lines.

Since any $2 \times 2$ matrix can be expanded in terms of Pauli matrices and the identity [24], then we lose no generality by considering errors $E \in G_n$. Because of this consideration, an error $E$ either commutes or anti-commutes with the elements of $S$. There are three situations then:

- If $E \in S$, the error commutes with all elements of $S$ and, moreover, it does not alter at all the encoded information (Equation (2.29)), and thus there is nothing to correct.
- If $E \notin S$ and it does not commute with all the elements of $S$, then $E$ is a *correctable* error, it will anti-commute $ES_i = -S_iE$ with some elements of $S$ taking the original state to an orthogonal one which can be detected and corrected.
- If $E \notin S$ but it does commute with all the elements of $S$, then it will take an state inside $V_S$ to another of the states of this set. This is problematic because then $E$ is a, so called *uncorrectable* error, and thus it can not detected and corrected.

The centralizer $Z(S)$ of $S$ is defined as the set of operators that commute with the generators $S_i$. Using this definition, we can identify the correctable errors of code $C(S)$ as the set $E_c = \{E_k\}$ for which $E_j^\dagger E_k \notin Z(S) - S$[6] holds for all $j$, and $k$.

[6] Notice that $Z(S) - S$ is the set of operators which commute with the generators $S_i$ but that are not the generators themselves.

We have just established which errors can be corrected. We are going to use the three-qubit code to exemplify all this, but before that we finish the presentation of stabilizer codes by explaining how we can detect correctable errors and correct them.

For syndrome measurement we are going to use an operator that projects the state of the system onto the space of the generators.

$$P = \frac{\prod_{j=1}^{n-k} (I + S_j)}{2^{n-k}}. \tag{2.32}$$

Then, when the eigenvalue of each of the generators $S_i$ is $1$, we get $P = 1$. But if one or more eigenvalues of $S_i$ is $-1$, we get $P = 0$.

In practice syndrome extraction is done by measuring each of the generators in a rapid sequence. In this way, we obtain values $\beta_i = \pm 1$ associated with each measurement, such that $E_j S_i E_j = \beta_i S_i$. In case we obtain $\beta_i = -1$ for some $i$, we can proceed to apply the operator $E_i^\dagger$ to correct the error that occurred. This process will become clearer when we apply it to our canonical example of the three-qubit code below.

The last concept we will introduce is the *code's distance*. This distance is important since it tells us how many errors can the code correct.

The code's distance is calculated using the error's *weight* $|E_k|$. To understand what is the weight of an error operator we recall their definition, Equation (2.13): an error operator $E_k \in G_n$ is written in terms of a tensor product of operators which can be Pauli $x$, $y$, $z$ matrices or the identity. Then error's weight is simply the number of its factors which are not the identity.

Finally, the code's distance is the minimum weight of one of the uncorrectable errors, i.e. $E_k \in Z(C) - S$:

$$d = \min_{E_k \in Z(C) - S} |E_k| . \tag{2.33}$$

As we said, the code's distance indicates how many errors can it correct: we need the code's distance to be, at least, $d = 2t + 1$ such that it can correct $t$ errors [3].

### Very simple example: three-qubit bit flip code

Let us use our go-to example to illustrate the concepts we just presented.

As we said before, the stabilizer's generators in this case are $S = \langle \sigma^z \sigma^z I, \sigma^z I \sigma^z \rangle$, which

| $\sigma^z\sigma^z I$ | $\sigma^z I\sigma^z$ | Error type | Action |
|---|---|---|---|
| $+1$ | $+1$ | no error | $III$ |
| $+1$ | $-1$ | qubit 3 flipped | $II\sigma^x$ |
| $-1$ | $+1$ | qubit 2 flipped | $I\sigma^x I$ |
| $-1$ | $-1$ | qubit 1 flipped | $\sigma^x II$ |

Table 2.2: Error detection and correction. Adapted from [3].

through the condition $S_i|\psi\rangle = |\psi\rangle$ specify the codewords $|000\rangle$, and $|111\rangle$.

The errors in this case are constituted by $x$ Pauli matrices, since we are working only with bit-flip errors. Errors then form the set:

$$E = \{III,\, \sigma^x II,\, I\sigma^x I,\, II\sigma^x,\, \sigma^x\sigma^x I,\, \sigma^x I\sigma^x,\, I\sigma^x\sigma^x,\, \sigma^x\sigma^x\sigma^x\}\,. \tag{2.34}$$

As we saw, the correctable errors anti-commute with one or more generators. It can be readily verified that these are given by the set:

$$E_c = \{III,\, \sigma^x II,\, I\sigma^x I,\, II\sigma^x,\, \sigma^x\sigma^x I,\, \sigma^x I\sigma^x,\, I\sigma^x\sigma^x\}\,.$$

Uncorrectable errors are the ones that commute with generators, but are not themselves generators (i.e. they belong to the set $Z\,(S) - S$). For the three-qubit bit-flip code, only $\sigma^x\sigma^x\sigma^x$ belongs to this category.

Since we have only one uncorrectable error with weight $|E| = 3$, the code's distance is $d = 3$, and it can correct errors in just $t = 1$ qubit.

Finally, to do syndrome extraction and correction we measure the generators and correct accordingly. This actions are condensed in Table 2.2.

This analysis does not bring up anything new for this particular code, but it certainly helps illustrate stabilizer codes. This makes introducing the surface code, an specific type of stabilizer code, a more straightforward task.

## 2.4 Surface code

The surface code is an stabilizer code $C\,(S)$ constructed on an square lattice with spins located on its links [25, 26]. It is several important features: 1) first it has a very high threshold [27, 28, 29]; 2) its two-dimensional geometry allows for an easy access to individual qubits (by the electronic components necessary to control them); and finally 3) it requires

only local gates and measurements. Due to this impressive list of features, it has been actively researched for experimental implementation[30, 31].

Having justified our election for surface codes, let us now introduce their elements. The surface code's generators, called simply stabilizer operators in the literature, are *star* $A_s$ and *plaquette* $B_p$ operators:

$$A_s = \prod_{j \in s} \sigma_j^x \text{ and } B_p = \prod_{j \in p} \sigma_j^z. \tag{2.35}$$

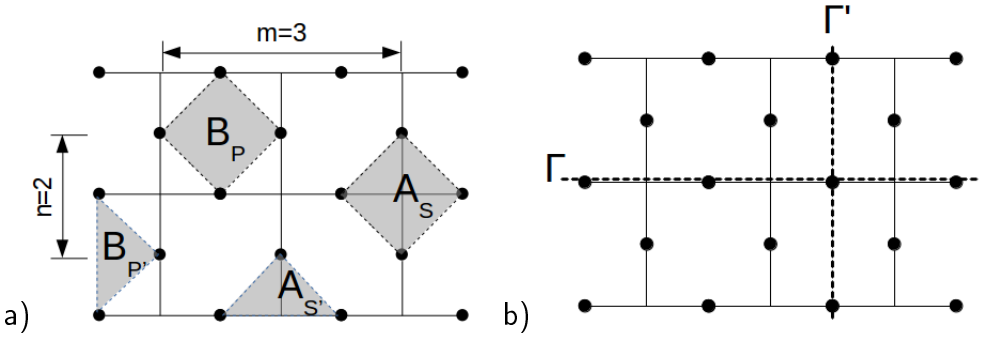


Figure 2.5: Surface code

Star operators are located around vertexes $s$, and plaquette operators are located on the faces $p$ of the lattice, see Figure (2.5).

It can be easily seen that all the stabilizer operators commute, as is expected:

$$[A_s, B_p] = [A_s, A_{s'}] = [B_p, B_{p'}] = 0. \tag{2.36}$$

Stars commute between them trivially and the same holds for plaquettes. Stars and plaquettes commute between them since they share either none or two qubits.

We label $n \times m$ a lattice (Figure (2.5)) which has $nm$ total vertical links, and $(n+1)(m+1)$ total horizontal links. Since there is a qubit in each link, we have

$$n_{\text{total}} = 2mn + m + n + 1 \tag{2.37}$$

qubits in the lattice.

On the other hand there are $(n+1)m$ star operators, and $n(m+1)$ plaquette operators. This amounts to having

$$k = 2nm + n + m \tag{2.38}$$

generators total. Recalling Section 2.3.2, we conclude this code supports $n_{\text{total}} - k = 1$ logical qubits.

More qubits can be stored in a single lattice by relaxing the stabilizer constrain. Another approach proposed in the literature is to have finite patches of a plane (each one encoding a logical qubit) and when necessary attach these patches by turning on qubits and stabilizers connecting them. As we mentioned before, the fact that the surface code has one of the largest error thresholds (as well as its other advantages) makes it possible that these patches could in principle be quite small.

The protected space $V_S$ is defined by the stabilizer formalism as the set of common eigenstates of the stabilizer operators, i.e.:

$$V_S = \{|\psi\rangle \in \mathcal{H} \,:\, A_s|\psi\rangle = |\psi\rangle,\, B_p|\psi\rangle = |\psi\rangle \text{ for all } s,\, p\}\,, \tag{2.39}$$

where $\mathcal{H}$ is the complete Hilbert space of all the qubits of the lattice.

The surface code's codewords are:

$$\left|\bar{\uparrow}\right\rangle = G\left|\Omega\right\rangle, \tag{2.40}$$

$$\left|\bar{\downarrow}\right\rangle = \bar{X}\left|\bar{\uparrow}\right\rangle, \tag{2.41}$$

where $|\Omega\rangle$ is the ferromagnetic state ($\sigma_j^z\,|\Omega\rangle = +\,|\Omega\rangle$ for all $j$), $G = \frac{1}{\sqrt{2^{N_g}}}\prod_s (1 + A_s)$, and $\bar{X}$ is a *logical operator*, which consists of a string of $\sigma^x$ operators acting in physical qubits and it goes from the top to the bottom edge of the lattice, e.g. path $\Gamma'$ from Figure 2.5-b:

$$\bar{X} = \prod_{j\in\Gamma'} \sigma_j^x. \tag{2.42}$$

The other logical operator possible is $\bar{Z}$, a string of $\sigma^z$ operators which goes from one side of the lattice to the other, e.g. path $\Gamma$ from Figure 2.5-b:

$$\bar{Z} = \prod_{j\in\Gamma} \sigma_j^z. \tag{2.43}$$

Both of those logical operators, when induced by the environment, constitute uncorrectable errors. This is because they commute with all the elements of the stabilizer and consequently they are not detected when syndrome extraction is performed.

We recall now the concept of the code's distance (Equation (2.33)), defined by the weight of the smallest uncorrectable error. Since for the surface code those errors are $\bar{X}$ and $\bar{Z}$, the code's distance will correspond to the shortest path between the top and bottom or the left and right edges of the lattice, for an $n \times m$ lattice this is $d = \min\{n+1, m+1\}$. Then the surface code can correct $\lfloor (d-1)/2 \rfloor$ errors.

### 2.4.1 Surface code's error threshold

An early calculation of the surface code's error threshold is presented by Dennis et. al. in [26]. They consider uncorrelated, stochastic errors and they map the problem of finding the surface code's accuracy threshold to one involving finding the critical point of an equivalent spin system.

They study two cases: in the first one it is assumed that the syndrome extraction is perfectly performed in one time step (i.e. the errors detected correspond exactly to the errors that happened in our system, i.e. no experimental errors intervened in our measurements). In the second case they take into account possible experimental errors in the syndrome extraction process, so that syndrome extraction has to be performed various times (i.e. during various time steps).

The first case (perfect syndrome extraction) lead Dennis et. al. to an equivalent spin system in two dimensions (actually a random bond Ising model), where the error threshold $p_c = 0,1094 \pm 0,0002$ corresponds to the critical point on the Nishimori line.

The second case (imperfect syndrome extraction) lead them to an spin system in three dimensions (a $Z_2$ gauge theory with quenched randomness) in which the third dimension corresponds to the time during which the various syndrome extractions occur. Again the error threshold is related to the critical point of the model on the Nishimori line. Here they only could obtain a lower bound of $p_c \geq 0,0114$.

Some later calculations of the error threshold of the surface code were performed using stochastic error models and mapping the problem onto an equivalent spin model [32, 33].

Another type of determination of the accuracy threshold involves developing algorithms for determining error recovery procedure from the information obtained by the syndrome extraction

[29, 34]. In this approach, stochastic errors happening in a quantum memory are simulated in a computer. Then the final state of the simulation is passed on to an algorithm that will determine how the recovery should be performed. The percentage of times that the algorithm got the recovery procedure right corresponds to the accuracy threshold. These estimates lead to lower values for the threshold, related to the difficulty of properly identifying the errors.

We leave the discussion of the accuracy threshold in relation to other kinds of error models for Section 3.5.

# Chapter 3

# Open quantum systems

Quantum systems that interact with their environment are called open quantum systems, in contrast to closed quantum systems which are the ones that do not interact with their surroundings. In this sense, quantum computers are indeed open quantum systems.

The study of open quantum systems began well before Quantum Information entered the research mainstream [35, 36], but since then it has been increasingly relevant to understand their dynamics because experimental applications depend upon this knowledge.

In the previous Chapter, we presented methods for protecting a quantum memory from the pervasive effects of its interaction with the environment. We also stated that theoretical study of those methods has traditionally assumed stochastic error models.

In this Chapter we are going to explain in more detail what these stochastic error models are and what are their downsides. We are also going to study the system plus reservoir approach, a broader framework for studying the dynamics of open quantum systems. We will also show that stochastic error models constitute an special case of the system plus reservoir approach (weak coupling).

Then we will present the spin-boson model. This model is constituted by a two level system interacting with an infinite set of harmonic oscillators. This model has the advantages of being exactly solvable and presenting characteristics like non-Markovianity, which are not captured by stochastic error models.

Finally, we revisit the threshold theorem and show how it is modified when this different environmental models are taken into account.

## 3.1 System plus reservoir approach

The starting point of this approach is to consider that the system of interest $S$ (e.g. the quantum memory) and its environment $B$ (also called bath or reservoir)[1] form closed total system $S+B$. This means that this total system evolves unitarily [14, 3, 13]. We also call $S$ and $B$ sub-systems of the total system.

The total system's Hilbert space is given by the tensor product of the system's and bath's Hibert spaces, i.e. $\mathcal{H}_S \otimes \mathcal{H}_B$, and the total Hamiltonian as a function of time is [14]:

$$\begin{aligned} H(t) &= H_S \otimes I_B + I_S \otimes H_B + H_I(t) \\ &= H_S + H_B + H_I(t), \end{aligned} \tag{3.1}$$

where $H_S$, $H_B$, and $H_I$ are the Hamiltonian of the system, of the bath, and of the interaction system-bath. $I_S$, and $I_B$ are the identity operators in the Hilbert space of the system and of the bath. We did not write the tensor products in the last line just to simplify the notation.

The state of a quantum system is represented in introductory approaches by its wave function, e.g. in the coordinate space, $\Psi(\vec{r})$ or by its state using Dirac notation $|\Psi\rangle$. But the most general approach to represent the state of a quantum system is through its density matrix $\rho$.

When the system is in a pure state $|\Psi\rangle$, the density matrix is simply $\rho = |\Psi\rangle\langle\Psi|$. But a density matrix is equally adequate for representing an statistical mixture $\rho = \sum_a w_a |\psi_a\rangle\langle\psi_a|$, for some set of states $\{|\psi_a\rangle\}$ and a set of weights $\{w_a\}$, which meet the condition $\sum_a w_a = 1$. More on the density matrix can be found in [14].

Since the total system is closed its evolution could be calculated in principle using the total Hamiltonian $H(t)$ and the standard Schrödinger and Heisenberg equations. For instance, if the initial state (at time $t_0$) of the total system is a pure state $|\psi(t_0)\rangle$, then its time evolution follows the Schrödinger equation:

$$i\frac{d}{dt}|\psi(t)\rangle = H(t)\,|\psi(t)\rangle. \tag{3.2}$$

The solution to this equation is given by an evolution operator $U(t, t_0)$ so that the state of

[1] We are going to use the names environment, bath, and reservoir interchangeably. The label $B$ for the bath is contingent.

the system as a function of time is given by

$$|\psi(t)\rangle = U(t,t_0)\,|\psi(t_0)\rangle. \tag{3.3}$$

Thus, the explicit expression for the evolution operator is obtained by solving the equation:

$$i\frac{\partial}{\partial t}U(t,t_0) = H(t)\,U(t,t_0)\,. \tag{3.4}$$

And the solution to this equation involves a time ordered $T_t$ exponential:

$$U(t,t_0) = T_t e^{-i\int_{t_0}^{t} H(t')\cdot dt'}. \tag{3.5}$$

## Dyson series and Magnus expansion

The evolution operator in general is difficult to calculate, so there are different expansions, like the Dyson series or the Magnus expansion, that can be used to obtain truncated, but workable, expressions. We present briefly two of these expansions here, following Chapter 1 of [11].

The Dyson series is an infinite sum,

$$U(t) = I + \sum_{n=1}^{\infty} S_n(t)\,, \tag{3.6}$$

where each of its terms involves time-ordered integrals:

$$S_n(t) \equiv (-i)^n \int_0^t dt_1 H(t_1) \int_0^{t_1} dt_2 H(t_2) \ldots \int_0^{t_{n-1}} dt_n H(t_n)\,. \tag{3.7}$$

Notice that time ordered here means that the earlier time integral is at the utmost right, and later times follow to its left sequentially.

If the Hamiltonian is time-independent each of these terms become $S_n(t) = (-iHt)^n/n!$, then the evolution operator takes the familiar form $U(t) = e^{-iHt}$.

On the other hand, the Magnus expansion at a time $t$ is an operator series

$$\Omega(t) \equiv \sum_{n=1}^{\infty} \Omega_n(t)\,,$$

where $\Omega_n(t)$ is $n$th order in the Hamiltonian $H(t)$ and we write the lowest orders explicitly below.

In the evolution operator this series appears in the exponential, though, $U(t) = e^{\Omega(t)}$. In this case we have an interesting property: if we take a fixed time $T$, then we can define an effective time-independent Hamiltonian $H_{eff} = \frac{i}{T}\Omega(T)$ which generates an equivalent time evolution to the one generated by the time-dependent Hamiltonian.

The terms of the Magnus expansion do not have a simple closed formula like the Dyson series' ones. In general they can be obtained using a recursive formula. Here we write the first three terms of the Magnus expansion:

$$\Omega_1(t) = -i\int_0^t dt_1 H(t_1), \tag{3.8}$$

$$\Omega_2(t) = -\frac{1}{2}\int_0^t dt_1 \int_0^{t_1} dt_2 \left[H(t_1), H(t_2)\right], \tag{3.9}$$

$$\Omega_3(t) = -\frac{1}{6}\int_0^t dt_1 \int_0^{t_1} dt_2 \int_0^{t_2} dt_3 \left(\left[H(t_1), \left[H(t_2), H(t_3)\right]\right] + \left[H(t_3), \left[H(t_2), H(t_1)\right]\right]\right). \tag{3.10}$$

Although generating terms of arbitrary order is easy with the Dyson series and its convergence is granted if $H$ is a bounded operator for all $t$, a truncation of the series does not leads to an unitary operator.

The Magnus expansion converges if $\int_0^t dt' \|H(t')\| < \pi$, but it may not do it otherwise. As we said its terms do not have a general form, but this expansion is unitary order by orders. Hence a truncation of the series will produce an unitary operator.

## Reduced density matrix

Although the evolution operator will be a key ingredient for our later analysis, the evolution of the $S+B$ system as a whole is not actually what we are interested in: we want to investigate what is the effect of the bath on the system of interest. To that end we use the concept of reduced density matrix.

In order to obtain the reduced density matrix of a sub-system, we "trace out" the other system's degrees of freedom [11, 3]. So if $\{|\phi_{B,i}\rangle\}$, $i = 1, 2, ..., n_B$, is the complete set of the bath's states, then $\rho_S = \mathrm{tr}_B\rho = \sum_{i=1}^{n_B}\langle\phi_{B,i}|\rho|\phi_{B,i}\rangle$ is the reduced density matrix of the

system of interest. Then the time evolution of the system of interest is given by [14]:

$$\rho_S(t) = \mathrm{tr}_B\left\{U(t,t_0)\,\rho(t_0)\,U^\dagger(t,t_0)\right\}, \tag{3.11}$$

We can also be interested in calculating the mean value of some observable represented by the operator $O$. An operator in the space of the system of interest takes the form $O_S = O_S \otimes I_B$, and its mean value can be calculated in the following way:

$$\langle O\rangle = \mathrm{tr}_S\left\{O\rho_S(t)\right\}. \tag{3.12}$$

Calculating this density matrices, and manipulating operators is by no means a trivial task. That is why there are multiple methods to deal with the specific features of open quantum systems. The Feynman-Vernon path integral approach [12, 13], master equations [14], and stochastic error models [14, 15].

In the following Section, we introduce the master equations approach, which involves making the Born-Markov approximation that limits it to weak couplings between the environment and the system of interest. We also describe briefly what stochastic error models are.

We want to emphasize that master equations and stochastic error models are very useful for studying a particular and important case. Also they are advantageous because their mathematical manipulation is relatively easier than other methods. Finally, a lot of important results, like the traditional form of the threshold theorem, have derived from their study. But if we want to prove a little further the topic of open quantum systems we will need to go beyond the master equations and stochastic error models.

## 3.2 Weak coupling

A widely used method for dealing with this regime is the one involving quantum master equations [11, 14]. The goal here is obtaining first-order linear differential equations that describe the dynamics of an open quantum system, in the same spirit of the Schrödinger equation. Quantum master equations propagate density matrices to density matrices, though, not pure states to pure states like the Schrödinger equation does.

In the following lines we describe how the derivation of the Markovian quantum master equation is done. This is a master equation which involves the Born-Markov approximation and

it is time local (it only depends on the density operator at present time, without retarded terms). From these approximations follow the main Markovian master equation's main advantages which are that the resulting equation is numerically and analytically tractable. But also they constitute the main limitation of this approach: its applicability is limited to the specific conditions we mentioned.

There are various ways to get to the Markovian master equation, we are going to follow Breuer and Petruccione's microscopic derivation of the equation [14] (Chapter 3).

We write the total Hamiltonian as we did before, Equation (3.1): $H = H_S + H_B + H_I$. And we start from the von Neumann equation in the interaction picture:

$$\frac{d}{dt}\rho\left(t\right) = -i\left[\hat{H}_I\left(t\right), \rho\left(t\right)\right], \tag{3.13}$$

and its integral form $\rho\left(t\right) = \rho\left(0\right) - i\int_0^t ds\left[\hat{H}_I\left(s\right), \rho\left(s\right)\right]$.

Inserting the integral equation into the von Neumann equation and taking the trace over the bath we get:

$$\frac{d}{dt}\rho_S\left(t\right) = -i\int_0^t ds \mathrm{tr}_B\left[\hat{H}_I\left[\hat{H}_I\left(s\right), \rho\left(s\right)\right]\right], \tag{3.14}$$

assuming $\mathrm{tr}_B\left[\hat{H}_I\left(s\right), \rho\left(0\right)\right] = 0$, since we are only interested in first-order terms in this approach.

Now we start with the approximations, the first one we perform is the Born approximation. We assume that the density matrix of the environment is negligibly affected by the interaction with the system, i.e. $\rho\left(t\right) \approx \rho_S\left(t\right) \otimes \rho_B$. Then the von Neumann equation becomes:

$$\frac{d}{dt}\rho_S\left(t\right) = -i\int_0^t ds \mathrm{tr}_B\left[\hat{H}_I\left(t\right)\left[\hat{H}_I\left(s\right), \rho_S\left(t\right) \otimes \rho_B\right]\right]. \tag{3.15}$$

This is the so called Redfield equation. It is local in time but it is not a Markovian master equation yet since it still depends upon the initial conditions. In order to solve this inconvenience, we make one more manipulation: we substitute $s$ by $t-s$ in the integral and let the upper limit of the integral go to infinity. It is possible to do this if the integrand disappears sufficiently fast for $s \gg \tau_B$, where $\tau_B$ is the time scale over which the reservoir correlation functions decay. Thus the Markov approximation is justified for $\tau_R \gg \tau_B$, i.e. the time scale over which the state of the systems varies appreciably $\tau_R$ is far greater than the relevant time scale for the bath's correlation functions $\tau_B$.

Performing this substitution, we finally obtain the Markovian quantum master equation:

$$\frac{d}{dt}\rho_S(t) = -i\int_0^\infty ds \mathrm{tr}_B\left[\hat{H}_I(t)\left[\hat{H}_I(t-s), \rho_S(t)\otimes\rho_B\right]\right] \tag{3.16}$$

Notice that this approximation implies that the correlation time $\tau_B$ is not resolved, thus we say the that the time axis is coarse-grained. This is the Born-Markov approximation.

It is also desirable to work a little bit more on this equation so it defines the generator of a dynamical semigroup. This guarantees that the evolution will be completely positive and trace preserving.

To accomplish this, we perform the rotating wave approximation. This involves averaging over the rapidly oscillating terms in the master equation. But first we need to write some of the equation's terms in a different manner. The Schrödinger picture interaction Hamiltonian can be written in its more general form in the following way:

$$H_I = \sum_\alpha A_\alpha \otimes B_\alpha,$$

where $A_\alpha^\dagger = A_\alpha$ and $B_\alpha^\dagger = B_\alpha$. And it can rewritten as:

$$H_I = \sum_{\alpha,\omega} A_\alpha(\omega)\otimes B_\alpha = \sum_{\alpha,\omega} A_\alpha^\dagger(\omega)\otimes B_\alpha^\dagger,$$

where $\omega = \epsilon - \epsilon'$, and $\epsilon$ and $\epsilon'$are energy eigenvalues of the system.

Using this, and through some manipulation [14], we get to the equation:

$$\frac{d}{dt}\rho_S(t) = -i[H_{LS}, \rho_S(t)] + \mathcal{D}(\rho_S(t)). \tag{3.17}$$

The Hamiltonian contribution to the dynamics is given by the Hermitian operator

$$H_{LS} = \sum_\omega \sum_{\alpha,\beta} S_{\alpha\beta}(\omega) A_\alpha^\dagger(\omega) A_\beta(\omega), \tag{3.18}$$

and the dissipator is

$$\mathcal{D}(\rho_S) = \sum_\omega \sum_{\alpha,\beta} \gamma_{\alpha\beta}(\omega)\left(A_\beta(\omega)\rho_S A_\alpha^\dagger(\omega) - \frac{1}{2}\left\{A_\alpha^\dagger(\omega)A_\beta(\omega), \rho_S\right\}\right). \tag{3.19}$$

Diagonalizing $\gamma_{\alpha\beta}$ we obtain the Lindblad form. $\gamma_{\alpha\beta}(\omega)$ and $S_{\alpha\beta}(\omega)$ are the real and imaginary parts of the Fourier transform of the bath correlation function:

$$\Gamma_{\alpha\beta}(\omega) = \frac{1}{2}\gamma_{\alpha\beta}(\omega) + iS_{\alpha\beta}(\omega) \equiv \int_0^\infty ds \cdot e^{i\omega s} \left\langle B_\alpha^\dagger(t) B_\beta(t-s) \right\rangle . \tag{3.20}$$

Let us sum up the weak-coupling limit in the following lines. The weak-coupling assumption lets us expand the exact equation of motion for the density matrix to first order. This assumption also suggests that the system and the bath's density matrices are approximately separable and the bath is almost not affected, i.e. $\rho(t) \approx \rho_S(t) \otimes \rho_B$. These two conditions make up the *Born approximation* to the master equation.

The quantum master equation is made local in time by replacing the density matrix $\rho_S(s)$ at the retarded time $s$ with the one at the present time $\rho_S(t)$. This is the *Markov approximation*.

The integration limit is pushed to infinity to get the *Born-Markov approximation* of the master equation and the relevant physical condition for this approximation is that the bath correlation time $\tau_B$ is small compared to the relaxation time of the system, i.e. $\tau_B \ll \tau_R$.

One last common approximation is done by neglecting rapidly oscillating terms proportional to $e^{i(\omega'-\omega)t}$ for $\omega' \neq \omega$. This is the rotating wave approximation, and it leads to the master equation in the *Lindblad form*. This amounts to the inverse frequency differences involved in the problem being small compared to the relaxation time of the system, i.e. $\tau_S \sim |\omega' - \omega|^{-1} \ll \tau_R$.

## 3.3 Stochastic error models

This is the last kind of model for the description of open quantum systems we are going to touch on. As we have been stating, it is also widely used in the quantum error correction literature due to its simplicity [11, 3]. The basic ingredient for this models is a basic set of errors, represented by operators $\{E_i\}$ which multiply the state of system $|\psi\rangle \to E_i|\psi\rangle$. If this operators are not unitary, the state of the system needs to be normalized after the action of an error operator.

It is also assumed that this errors occur at some fixed rate $r_i$, as a Poisson process. Then the probability of an error $E_i$ occurring in a time interval $\Delta t$ is $p_i = r_i \Delta t$. For the case of quantum error correction it is needed that $r_i$ is small, as we saw in Chapter 2.

Depolarizing noise is a typical example of this kind of model used in quantum error correction. Here each qubit is multiplied by the Pauli operators $\sigma^x$, $\sigma^y$, and $\sigma^z$. If the rates of each

error is the same, $r/3$, then after a time $\Delta t$ depolarizing noise takes the initial density matrix $\rho$ for one qubit to [3]:

$$\rho(\mathcal{E}) = (1-p)\rho + \frac{p}{3}(\sigma^x\rho\sigma^x + \sigma^y\rho\sigma^y + \sigma^z\rho\sigma^z), \tag{3.21}$$

where $p = r\Delta t$.

After this brief presentation we just want to mention two results which are the most relevant for us. Their proof is beyond the scope of this work, for it we recommend the interested reader to Chapter 1 of [11]. First, discrete-time stochastic error models can be equivalent to some CPTP (completely positive trace-preserving) maps. And when we consider continuous time, the noise can be described by Markovian master equations.

This last result we want to emphasize, it means that stochastic error models are subject to the same validity conditions that we mentioned before.

## 3.4 Spin-boson model

Now that we established that the general system-plus-environment approach is the more adequate for the task of studying the dynamics of an open quantum system, and by extension of a quantum memory, we are going to concern ourselves on describing what exactly will our environment be.

A model for the environment should be simple enough so that analytical and numerical calculations are feasible but which captures the fundamental aspects of a real environment. The spin-boson model then fits nicely here: it meets our requirements and it has been extensively studied inside and outside the context of quantum information [13, 37].

In the spin-boson model the tunneling between states of a two-level quantum system is studied, e.g. an spin-$1/2$ particle, when it is coupled to a bath of harmonic oscillators. This kind of environment is justified by its spectral function [35], which lets us compare theoretical and experimental results.

At $T = 0$, it is possible to assume that the harmonic oscillator's bath is coupled linearly to the spin of the particle when the latter affects only weakly the former. Although this was not its original purpose, this model is particularly relevant for our analysis since it lets us investigate the effect of the environment on a qubit.

One important comment must be made before we move on studying this model, it has

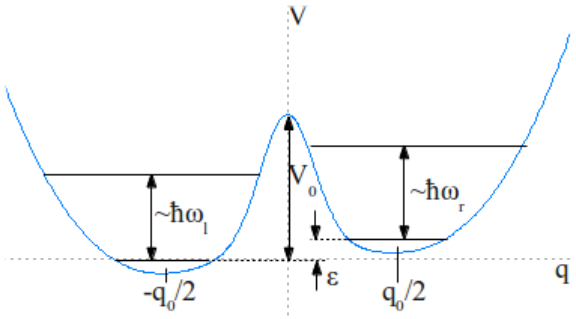


Figure 3.1: Two-wells separated by a potential barrier. $\hbar\omega_l$ and $\hbar\omega_r$ are the energy differences between the lowest and the first exited states of the left and right wells, respectively. $\varepsilon$ is the energy difference between the lowest state of the left and the right side.

to do with the two-level system. This system can be *intrinsically* limited to this two levels, like an spin-$1/2$ particle. But it can also be that we have a system in which there are only two relevant energy states because all others are not accessible by excitations due to thermal perturbations, for example. In this case we have a *truncated* two-level system.

The canonical truncated system is one which has one continuous degree of freedom $q$ (e.g. a particle moving in one spatial dimension) and it is constrained by two potential wells separated by a potential barrier $V_0$, Figure 3.1.

There are some conditions that a truncated two-level system needs to meet. Defining a frequency $\omega_0$ which is of the same order of magnitude as $\omega_l$ and $\omega_r$, we write those conditions:

$V_0 \gg \hbar\omega_0$, the potential barrier is much larger than the energy difference between the lowest and first excited energy states.

$k_BT \ll \hbar\omega_0$, the thermal energy is much smaller than the energy difference between the lowest and first excited energy states ($k_B$ is Boltzmann constant and $T$ is the temperature). This implies that thermal energy can not take the system to an excited state.

One important consequence of the fact that $V_0 \gg \hbar\omega_0$ for this truncated system is that the matrix element of the tunneling process between the wells, $\hbar\Delta_0$, is exponentially small compared to $\hbar\omega_0$. Thus the tunneling do not mix the ground states with the excited states.

Now we are going to present formally the spin-boson model. First we are going to study the classical version of the model, as is customary in the literature [12, 13, 36]. The quantum version, which is obtained in an straightforward manner from the classical one, is presented after that.

Let us start introducing the classical case by considering only the two-level system, i.e. isolated from its environment. Later on we will introduce the coupling between them, but for now the Hamiltonian of the system is:

$$H_{TSS} = -\frac{1}{2}\hbar\Delta_0\sigma^x + \frac{1}{2}\epsilon\sigma^z, \tag{3.22}$$

where $\sigma^x$ and $\sigma^y$ are the Pauli matrices, as usual. We chose a basis for the states of the system in which the eigenvalues of the $\sigma^z$ matrix coincide with the system's position. Then if the system is localized on the right-hand side, the correspondent eigenvalue is $+1$, and when it is localized on the left-hand side the eigenvalue is $-1$.

The dynamics of the system are given then by oscillations between the ground states of the left and right-hand wells. To illustrate this behavior we can look at the probability $P(t) = P_r(t) - P_l(t)$, where $P_r$ and $P_l$ are the probabilities of the system be on the right-hand or left-hand side well. Assuming $P(0) = 1$, we have:

$$P(t) = \cos\left[\sqrt{\epsilon^2 + (\hbar\Delta_0)^2}\cdot t\right]. \tag{3.23}$$

Now we consider the full system, system of interest plus environment. We have the contribution of the isolated system, the one from the harmonic oscillators, and the one coming from the interaction system-environment:

$$\begin{aligned} H &= H_{TSS} + H_{HO} + V \\ &= -\frac{\hbar\Delta\sigma^x}{2} + \frac{\varepsilon\sigma^z}{2} + \sum_\alpha\left(\frac{m_\alpha\omega_\alpha^2 x_\alpha^2}{2} + \frac{p_\alpha^2}{2m_\alpha}\right) + \frac{q_0\sigma^z}{2}\sum_\alpha C_\alpha x_\alpha, \end{aligned} \tag{3.24}$$

this is the spin-boson Hamiltonian. $H_{TSS}$ was defined in Equation (3.22), $H_{HO} = \sum_\alpha\left(\frac{m_\alpha\omega_\alpha^2 x_\alpha^2}{2} + \frac{p_\alpha^2}{2m_\alpha}\right)$ is the harmonic oscillators' Hamiltonian, and $V = \frac{q_0\sigma^z}{2}\sum_\alpha C_\alpha x_\alpha$ is the interaction term. Here $\Delta$ is analogous to $\Delta_0$ but renormalized for high-frequency effects. The variables $p_\alpha$, $m_\alpha$, $x_\alpha$, and $\omega_\alpha$ are the momentum, mass, position, and frequency of the $\alpha$-th harmonic oscillator of the bath. $\pm q_0/2$ are the positions of the minimum of the potential well (see Figure 3.1). $C_\alpha$ is the coupling of the system to the $\alpha$-th harmonic oscillator.

If we assume thermal equilibrium as the initial condition, we can codify the complete information about the environment in an *spectral function* $J(\omega)$, defined by the expression:

$$J(\omega) \equiv \frac{\pi}{2} \sum_{\alpha} \frac{C_{\alpha}^{2}}{m_{\alpha}\omega_{\alpha}} \delta(\omega - \omega_{\alpha}) . \tag{3.25}$$

This spectral function has a high-frequency cutoff, given by frequency $\omega_c$. This cutoff can be introduced in various forms, one of them is integrating over frequency from $\omega = 0$ to $\omega = \omega_c$ instead of integrating to $\omega \to \infty$. Thus we avoid divergences coming from integrating over all frequencies. Another way to introduce the cutoff is taking the case where the spectral density behaves as a power law of the frequency and multiplying it by a function which decreases exponentially with the frequency too, as to avoid high-frequency contributions:

$$J(\omega) = A\omega^{s'} e^{-\omega/\omega_c}. \tag{3.26}$$

Here we use $s'$ instead of just plain $s$ to differentiate it from the parameter $s$ that will appear in the Hamiltonian used in Chapter 4, which is *not* the same.

Assuming this spectral density and strictly one spin interacting with the bosonic bath, we can identify three regimes related to the value of $s$:

$0 < s' < 1$, sub-ohmic case: for $T = 0$ the system is localized in the ground state of one of the wells and for $T \neq 0$ the system relaxes (becomes localized) at a rate proportional to $\exp\left[-(T_0/T)^{1-s'}\right]$, $T_0$ is a constant related to the parameters of the model.

$s' = 1$, ohmic case: here we redefine the spectral density as $J(\omega) = \eta\omega e^{-\omega/\omega_c}$. In this case, depending on the value of $\alpha \equiv \eta q_0^2/2\pi\hbar$, there exist various behaviors: $\alpha > 1$, $T = 0$ where the system is localized, and $\alpha = 1/2$ and any $T$, there is an exponential decay with $\pi\Delta^2/2\omega_c$.

$s' > 1$, super-ohmic case: the system shows damped oscillations.

It is usually convenient to introduce creation $a_\alpha$ and annihilation $a_\alpha^\dagger$ operators for the bosons. They follow the usual harmonic oscillator commutation relations, i.e., $\left[a_\alpha, a_{\alpha'}^\dagger\right] = \delta_{\alpha\alpha'}$. We can write then the momentum and position of the bosons in terms of these new operators as:

$$x_\alpha = \sqrt{\frac{\hbar}{2m_\alpha\omega_\alpha}} \left(a_\alpha + a_\alpha^\dagger\right), \text{ and } p_\alpha = \sqrt{\frac{\hbar m_\alpha\omega_\alpha}{2}} \left(a_\alpha - a_\alpha^\dagger\right). \tag{3.27}$$

And we can rewrite Equation (3.24) as:

$$H = H_{TSS} + \sum_{\alpha} \hbar\omega_{\alpha} a_{\alpha}^{\dagger} a_{\alpha} + \frac{\hbar}{2}\sigma^{z} \sum_{\alpha} f_{\alpha}. \tag{3.28}$$

Here $H_{TSS}$ does not change (Equation (3.22)), $\sum_{\alpha} \hbar\omega_{\alpha} a_{\alpha}^{\dagger} a_{\alpha} = H_{HO}$ where we have dropped the zero-point energy, and $\frac{\hbar}{2}\sigma^{z} \sum_{\alpha} f_{\alpha} = V$ where the function $f_{\alpha}$ codifies the effects of the environment:

$$f_{\alpha} = \lambda_{\alpha} \left( a_{\alpha}^{\dagger} + a_{\alpha} \right). \tag{3.29}$$

The function $\lambda_{\alpha}$ is related to the spectral function as $C_{\alpha}$ was previously:

$$G(\omega) = \sum_{\alpha} \lambda_{\alpha}^{2} \delta(\omega - \omega_{\alpha}) = \frac{q_0^2}{2\hbar} \sum_{\alpha} \frac{C_{\alpha}^{2}}{m_{\alpha}\omega_{\alpha}} \delta(\omega - \omega_{\alpha}). \tag{3.30}$$

As it can easily be seen, this spectral density $G(\omega)$ is related to the spectral density of the continuous model: $G(\omega) = (q_0^2/\pi\hbar)\, J(\omega)$.

## 3.5 Accuracy threshold and correlated environments

In the present Chapter, we introduced different approaches to tackle the problem of modeling the interaction of quantum systems with their environment. We gave some arguments to illustrate why stochastic error models, which are standard in the study of quantum error correction, are only valid for weak coupling between the system and its environment.

For these reasons, we are going to focus on the remaining of this work on performing a more appropriate determination accuracy threshold (introduced in Sections 2.2 and 2.4.1), by starting from a phenomenological model similar to the spin-boson model, to account for the environment of the quantum memory. We also call this kind of environmental models *correlated* since errors are not independent, as in stochastic models, but they show correlations between them.

This Section tries to build a bridge between the stochastic and the correlated approaches to the error threshold, following Novais, Mucciolo and Baranger's (NMB) work (Chapter 25 of [11]).

At the heart of this problem lies the fact that it is not possible to define local error probabilities from correlated models [15]. Sometimes operator norms are used to characterize correlated environments [38], but they are not good parameters since some interacting Hamiltonians can

have large norms although the system-environment coupling is not strong.

NMB assume a general interaction term with the following form:

$$V = \sum_{\mathbf{x}} \sum_{\alpha=\{x,y,z\}} \frac{\lambda_\alpha}{2} f_\alpha(\mathbf{x})\, \sigma_\alpha(\mathbf{x}). \tag{3.31}$$

Notice it is similar to the spin-boson Hamiltonian's (Equation (3.28)) interaction term, but there is a sum over all Pauli matrices.

The environment is assumed to be described by a free field theory, i.e. fluctuations are Gaussian and Wick's theorem can be used to calculate high-order correlation functions. Here two-point correlation functions decay as power laws:

$$\langle \Psi_{\text{env}} | f_\alpha(\mathbf{x}_1, t_1)\, f_\beta(\mathbf{x}_2, t_2) | \Psi_{\text{env}} \rangle \sim \mathcal{O}\left( \frac{1}{|\mathbf{x}_2 - \mathbf{x}_1|^{2\delta}}, \frac{1}{|t_2 - t_1|^{2\delta/z}} \right), \tag{3.32}$$

where $\delta$ is called scaling dimension and $z$ is called dynamical exponent.

With this basis NMB perform a calculation of the probability of a particular history of syndromes through a Dyson series. They find that the relevant correlation function for the bath is

$$\langle F_\alpha(\mathbf{x}_i, t_i)\, F_\alpha(\mathbf{x}_j, t_j) \rangle \sim \mathcal{O}\left( \frac{1}{|\mathbf{x}_i - \mathbf{x}_j|^{4\delta_\alpha}}, \frac{1}{|t_i - t_j|^{4\delta_\alpha/z}} \right), \tag{3.33}$$

where $F_\alpha$ is a function of $f_\alpha$. Also the condition

$$D + z - 2\delta_\alpha < 0 \implies \delta_\alpha > \frac{D+z}{2}, \tag{3.34}$$

where $D$ is the dimension of the bath, is required for the perturbative expansion to converge.

What this implies is that when this condition (Equation (3.34)) is met, it is possible to assign probabilities to the errors, as in stochastic models, thus the traditional version of the threshold theorem applies.

On the other hand, for $\delta_\alpha > (D+z)/2$ we cannot assert that quantum error correction is impossible. What can happen is that a non-perturbative version of the threshold theorem is possible up to some point where correlations are so strong that they now start to make it impossible to store and compute with quantum information.

NMB also associate this results to phase transition theory: Equation (3.34) defines what is know as upper critical dimension of the model and a phase diagram of the quantum computer

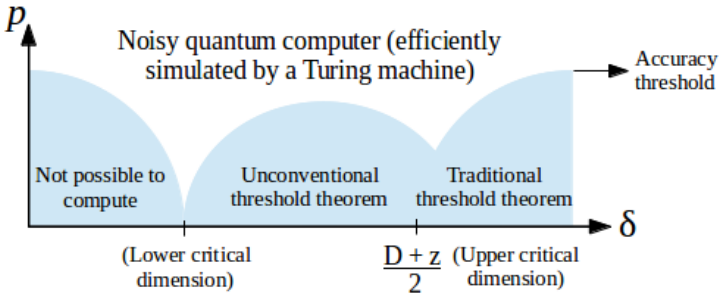


Figure 3.2: Phase diagram of a quantum computer running quantum error correction. Taken from [39].

can be drawn where one axis is given by the local error probability and the other is the scaling dimension of the environment. All this is summed up by Figure 3.2.

Following a similar approach, Khoon and Preskill obtained the same results in a later work [40].

### 3.5.1 Surface code's accuracy threshold and correlated environments

Novais, Mucciolo and collaborators have been working towards understanding the surface code when it is coupled to a correlated environment [16, 17, 41]. Up to now, they have investigated its time evolution over one error correction cycle.

In [16, 17, 41] they assume an interaction Hamiltonian which only induces bit-flips, i.e. it is similar to Equation (3.31) but only involving $\sigma^x$ terms. Using this model, the fidelity of the evolved state of the quantum memory with respect to its initial state is calculated.

The accuracy threshold is then calculated by mapping the problem to the order-disorder phase transition of an equivalent spin system, similarly to the works that we described in Section 2.4.1 which used stochastic error models. The presence of this threshold is confirmed by the fact that the fidelity can be made one by augmenting the size of the system, provided the coupling is below its critical value.

In the present case, it was also found that the critical temperature is inversely proportional to the coupling strength between the quantum memory and the environment and that the the threshold value is diminished to $p \sim 0,06$ even in the case of nearest neighbors effective interactions in an Ohmic environment.

In a later paper [17], a different interaction Hamiltonian is used. Here only some effective

interaction is assumed, without specifying its details:

$$H_{\text{eff}}\left(\{\sigma^x\}\right) = \sum_i h_i \sigma_i^x + \sum_{i \neq j} J_{i,j} \sigma_i^x \sigma_j^x, \tag{3.35}$$

where $h_i$ and $J_i$ codify the environmental details and can be real or imaginary numbers.

The method for solving the problem is again mapping the calculation of the fidelity (of the evolved state of the quantum memory with respect to the initial one) to the statistical mechanics problem of finding the phase transition of an equivalent spin system. The critical parameters were calculated analytically when the only first neighbors interactions are considered in the analogous spin system and numerically for greater correlations.

In this context, we can look at the next Chapter as an extension of these results, when a time evolution encompassing multiple quantum error correction cycles, instead of just one, is considered.

# Chapter 4

# Surface code in a correlated environment

Here we start putting together all the theory we presented in the previous Chapters. We study the time evolution of a quantum memory under the protection of the surface code (Chapter 2). To benchmark the protection, we calculate the fidelity of the evolved state of the memory, after $N$ error correction cycles, with respect to its initial state. The fidelity is a measure of the projection of an state $|\psi\rangle$ onto some reference state $|\psi_0\rangle$:

$$\mathcal{F} = \frac{\langle\psi|\psi_0\rangle\langle\psi_0|\psi\rangle}{\langle\psi|\psi\rangle}. \tag{4.1}$$

It is easy see that $0 \leq \mathcal{F} \leq 1$ and to interpret this measure:

- if $\mathcal{F} = 1$ then $|\psi\rangle = |\psi_0\rangle$, for us this means that the evolved state is the same as the one we encoded in the quantum memory, no information was lost, and
- if $\mathcal{F} = 0$ then $|\psi\rangle$ is orthogonal to $|\psi_0\rangle$, and the information we encoded is nowhere to be found.

Then, if $|\psi_0\rangle$ is the initial state of the system (memory plus environment) and $|\psi\rangle$ is its evolved state, it is evident that the closest we can keep the fidelity to one using quantum error correction, the more likely it is that our information can be maintained and successfully decoded.

We model the memory's interaction with its environment using a bosonic bath, as is done in the spin-boson model (Chapter 3). We consider the case of an environment initially at zero

temperature, $T = 0$, which is the regime where quantum correlations are more important.

Since the final goal here is to determine the error threshold of this memory (Chapter 2), we are going to assume the most favorable evolution possible for the success of the quantum error correction, i.e. we assume that all syndrome measurements return non-error values. This means that only uncorrectable errors could have occurred.

The accuracy threshold is calculated by mapping our dynamical problem onto a statistical mechanics one. As we have shown throughout this text, this is common-place.

## 4.1 Fidelity

The fidelity gives us an idea of "how far" one state is from another [3]. In this Section we are going to start calculating the fidelity of the evolved state of the system with respect to the initial state of our quantum memory $|\bar{\uparrow}\rangle\langle\bar{\uparrow}| \otimes I_{\text{environment}}$. This calculation will give us information about whether the state of our memory stays near its initial value or if it deviates substantially from it, in which case we could lose the quantum information codified in the memory.

For the initial state of the system, we assume that the quantum memory is not entangled with its environment, i.e. the total state is separable. This is a sound assumption since we should expect to be able to initialize the memory in any state we desire, otherwise it would not be useful as a computing device [3]. We also assume that the logical up state $|\bar{\uparrow}\rangle$ (Equation (2.40)) is encoded onto the memory:

$$|\psi_0\rangle = |\bar{\uparrow}\rangle \otimes |0\rangle. \tag{4.2}$$

With this initial state, the fidelity becomes:

$$\mathcal{F} = \frac{\langle\psi| \left(|\bar{\uparrow}\rangle\langle\bar{\uparrow}| \otimes I_{\text{environment}}\right) |\psi\rangle}{\langle\psi|\psi\rangle}, \tag{4.3}$$

and from now on we are not going to write explicitly $I_{\text{environment}}$.

### 4.1.1 Characterization of the environment

Since we are using the system plus reservoir approach and the environment is composed by bosons (or harmonic oscillators), the total Hamiltonian of the system plus the environment is:

$$H = H_0 + V = \sum_k \omega_k a_k^\dagger a_k + \lambda \sum_{\mathbf{r}} f(\mathbf{r}, t)\, \sigma_{\mathbf{r}}^x, \tag{4.4}$$

where:

$$H_0 = H_{\text{mem}} + H_{\text{bath}} = \sum_k \omega_k a_k^\dagger a_k, \tag{4.5}$$

$H_{\text{mem}} = 0$ is the memory's Hamiltonian (we assume the qubits do not interact between them) and $H_{\text{bath}} = \sum_k \omega_k a_k^\dagger a_k$ is the bath's Hamiltonian. The interaction term of the Hamiltonian is:

$$V = \lambda \sum_{\mathbf{r}} f(\mathbf{r}, t)\, \sigma_{\mathbf{r}}^x. \tag{4.6}$$

where $\lambda$ is a parameter determines the coupling strength between the bath and the system and $f(\mathbf{r}, t)$ is the bosonic operator:

$$f(\mathbf{r}, t) = \frac{(v/\omega_0)^{D/2+s}}{L^{D/2}} \sum_{\mathbf{k}\neq 0} |\mathbf{k}|^s \left( e^{+i\mathbf{k}\cdot\mathbf{r}+i\omega_k t} a_{\mathbf{k}}^\dagger + e^{-i\mathbf{k}\cdot\mathbf{r}-i\omega_k t} a_{\mathbf{k}} \right), \tag{4.7}$$

where $\omega_0$ is a characteristic microscopic frequency scale, $v$ is the propagation speed of excitations, and $D$ is the number of spatial dimensions of the environment. Here the creation and annihilation operators again follow the usual harmonic oscillator commutation relations, $\left[a_{\mathbf{k}}, a_{\mathbf{k}'}^\dagger\right] = \delta_{\mathbf{k}\mathbf{k}'}$. Also notice that $s$ here is not the same parameter that appears in the spin-boson model, and that is why we used $s'$ instead of $s$ when we presented it in Chapter 3.

The spectral function of this environment (see Chapter 3) can give us valuable information as to which concrete physical system our phenomenological model applies. We rewrite its expression here:

$$J(\omega) \equiv \frac{\pi}{2} \sum_k \frac{C_k^2}{m_k \omega_k} \delta(\omega - \omega_k), \tag{4.8}$$

where $C_k$ comes from the interaction term of the Hamiltonian:

$$V = q_0 \sigma_z \sum_k C_k q_k. \tag{4.9}$$

In order to calculate the spectral function for our model, we need to identify the expression for $C_k$. This is done by using Equations (4.6) and (4.7), and the relationship $q_k = \sqrt{\hbar/2m_k\omega_k}\left(a_k + a_k^\dagger\right)$. Also assuming $\omega_k = v\,|\mathbf{k}|$, we get:

$$C_k^2 = 2\lambda^2 \frac{(v/\omega_0)^{D+2s}}{q_0^2 L^D} m_k v k^{2s+1}. \tag{4.10}$$

Now we calculate the spectral density. We do this by inserting $C_k^2$ into Equation (4.8) and taking the continuum limit for $k$ ($\sum_k \to \frac{L^D}{(2\pi)^D}\int d^D k$). We also assume that the bath is two-dimensional (i.e. $D = 2$, which is the same dimensionality of the surface code lattice):

$$\begin{aligned} J(\omega) &= \frac{\lambda^2\pi}{(2\pi)^2}\frac{(v/\omega_0)^{2+2s}}{q_0^2}\int k dk \cdot d\theta \cdot k^{2s}\delta(\omega - \omega_k) \\ &= \frac{2\lambda^2}{q_0^2\omega_0^{2+2s}}\omega^{2s+1}, \end{aligned} \tag{4.11}$$

where we used the property $\delta(\omega - vk) = \delta\left(k - \frac{\omega}{v}\right)/v$.

### 4.1.2 Time evolution of the system

Now that we established the basic elements of our system, let us start constructing the quantities $\langle\psi|\bar{\uparrow}\rangle$ and $\langle\psi|\psi\rangle$ in order to calculate the fidelity.

The key here is the evolved state $|\psi\rangle$, this state is the result of alternating free evolutions (corresponding to the time between syndrome extractions) and projections (corresponding to the actual syndrome extractions):

$$|\psi\rangle = \mathcal{P}_0 U(N-1)\,\mathcal{P}_0 U(N-2)\ldots\mathcal{P}_0 U(2)\,\mathcal{P}_0 U(1)\,\mathcal{P}_0 U(0)\,|\bar{\uparrow}\rangle|0\rangle. \tag{4.12}$$

Notice that we are assuming that we can instantaneously measure error syndromes at the end of each error correction cycle and that the total evolution is *not* unitary due to the presence of the projection operators.

In the last expression there are two important quantities: the free-evolution operator $U(n)$ and the projection operator at the end of each cycle $\mathcal{P}_0$. Let us start writing the free-evolution operator. It is calculated using Equation (3.5) and the total Hamiltonian we have just written (Equation (4.4)). We also label each cycle of duration $\Delta$ with an integer $n \in [1,\, N]$, so that

it starts at time $(n-1)\,\Delta$ and ends at time $n\Delta$. All these facts lead us to:

$$U\left(n\right)=T_{t}e^{-i\lambda\int_{(n-1)\Delta}^{n\Delta}dt\sum_{\mathbf{r}}f(\mathbf{r},t)\sigma_{\mathbf{r}}^{x}}. \tag{4.13}$$

On the other hand, the projection operator at the end of each error correction cycle is simply:

$$\mathcal{P}_{0}=\prod_{P}\left(1+B_{P}\right)=|\bar{\uparrow}\rangle\langle\bar{\uparrow}|+|\bar{\downarrow}\rangle\langle\bar{\downarrow}|=|\bar{\uparrow}\rangle\langle\bar{\uparrow}|+\bar{X}|\bar{\uparrow}\rangle\langle\bar{\uparrow}|\bar{X}, \tag{4.14}$$

this operator projects the state onto the positive stars'[1] Hilbert space. We do not need to include the projector over the plaquettes, since our interaction couples the physical qubits only to $\sigma^{x}$ operators (bit flips), so no phase errors are induced by the environment. This certainly constitutes a simplification but it permits us to obtain analytic results. Also notice that since plaquettes are the dual of stars, our approach here is actually equivalent to a model which only takes into account phase errors under a duality transformation.

Working on the numerator of the fidelity and using the expression for the projection operator, we get:

$$\langle\psi|\left(|\bar{\uparrow}\rangle\langle\bar{\uparrow}|\right)|\psi\rangle=\sum_{\mathcal{KJ}}\langle0|\prod_{i=N-1}^{0}\langle\bar{\uparrow}|\mathcal{K}_{i}U^{\dagger}\left(i\right)\mathcal{K}_{i+1}|\bar{\uparrow}\rangle\prod_{i=0}^{N-1}\langle\bar{\uparrow}|\mathcal{J}_{i+1}U\left(i\right)\mathcal{J}_{i}|\bar{\uparrow}\rangle|0\rangle, \tag{4.15}$$

where $\mathcal{J}_{0}=\mathcal{K}_{0}=\mathcal{J}_{N}=\mathcal{K}_{N}=I$, $\sum_{\mathcal{KJ}}=\sum_{\mathcal{K}_{1},\ldots\mathcal{K}_{N-1}}\sum_{\mathcal{J}_{1}\ldots\mathcal{J}_{N}}$, and $\mathcal{J}_{i\neq0,N}=\mathcal{K}_{i\neq0,N}=\left\{I,\bar{X}\right\}$. We leave the details of the manipulations to Appendix A.1, because they are somewhat lengthy and add very little to our present discussion.

The denominator of the fidelity can be written in a similar way:

$$\langle\psi|\psi\rangle=\sum_{\mathcal{KJ}}\langle0|\prod_{i=N-1}^{0}\langle\bar{\uparrow}|\mathcal{K}_{i}U^{\dagger}\left(i\right)\mathcal{K}_{i+1}|\bar{\uparrow}\rangle\prod_{i=0}^{N-1}\langle\bar{\uparrow}|\mathcal{J}_{i+1}U\left(i\right)\mathcal{J}_{i}|\bar{\uparrow}\rangle|0\rangle, \tag{4.16}$$

where $\mathcal{J}_{0}=\mathcal{K}_{0}=I$, $\mathcal{K}_{N}=\mathcal{J}_{N}$, $\sum_{\mathcal{KJ}}=\sum_{\mathcal{K}_{1},\ldots\mathcal{K}_{N}}\sum_{\mathcal{J}_{1}\ldots\mathcal{J}_{N}}$, and $\mathcal{J}_{i\neq0}=\mathcal{K}_{i\neq0}=\left\{I,\bar{X}\right\}$. Again we skip the details here and we leave them to Appendix A.2.

Next we write the spin variables in the $x$ basis. Then instead of using $|\uparrow\rangle_{i}$ states we use $|+\rangle_{i}$ and $|-\rangle_{i}$ ones. These new states are such that $\sigma_{i}^{x}|\pm\rangle_{i}=\sigma_{i}|\pm\rangle_{i}$, where $\sigma_{i}=\pm1$. Then

[1] Stars or star operators are one of the surface code's stabilizer operators. See Section (2.4).

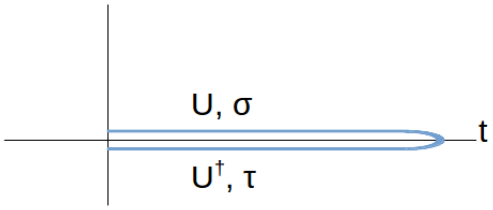


Figure 4.1: Keldysh contour.

we can re-write the ferromagnetic state as

$$|\Omega\rangle = \prod_i |\uparrow\rangle_i = \prod_i \left( \frac{|+\rangle_i + |-\rangle_i}{\sqrt{2}} \right) \tag{4.17}$$

and the logical up state (Equation (2.40)) as

$$|\bar{\uparrow}\rangle = G|\Omega\rangle = G \sum_\sigma |\sigma\rangle,$$

where we used the notation $|\sigma\rangle = |\sigma_1 \dots \sigma_N\rangle$. The same reasoning applies to the $\tau$ variables. We also assume that $U$ is diagonal in that basis, so that $UG = GU$.

Our attention returns now to the free-evolution operator. We are going to use the time-loop formalism, also known as the Keldysh formalism [11, 42, 43], in order to continue with our calculation. We think of the ket as moving forward in time (since it contains the operators of the form $U(n)$) and the bra moving backwards in time (since it contains the operators of the form $U^\dagger(n)$), as in the loop shown in Figure 4.1. In this approach, we need to use a different label for the spin variables for the forward and backward evolutions. We use the label $\sigma$ for the ket and $\tau$ for the bra.

Using the notation $u_i(\tau) = \langle s|U(i)|s\rangle$, where $s = \sigma, \tau$, the fidelity's numerator becomes:

$$\begin{aligned} \langle\psi| \left( |\bar{\uparrow}\rangle\langle\bar{\uparrow}| \right) |\psi\rangle = & \sum_{\tau,\sigma} \sum_{\mathcal{KJ}} \langle 0| \left[ \prod_{i=N-1}^{0} u_i^\dagger(\tau) \prod_{i=0}^{N-1} u_i(\sigma) \right] |0\rangle \\ & \times \prod_{i=N-1}^{0} \langle\tau|\mathcal{K}_i\mathcal{K}_{i+1}G|\tau\rangle \prod_{i=0}^{N-1} \langle\sigma|\mathcal{J}_{i+1}\mathcal{J}_i G|\sigma\rangle, \end{aligned} \tag{4.18}$$

where $\mathcal{J}_0 = \mathcal{K}_0 = \mathcal{J}_N = \mathcal{K}_N = I$, and $\mathcal{J}_{i\neq 0,N} = \mathcal{K}_{i\neq 0,N} = \left\{I, \bar{X}\right\}$. And its denominator is:

$$\langle\psi|\psi\rangle = \sum_{\tau,\sigma}\sum_{\mathcal{K}\mathcal{J}}\langle 0|\left[\prod_{i=N-1}^{0} u_i^{\dagger}(\tau)\prod_{i=0}^{N-1} u_i(\sigma)\right]|0\rangle \prod_{i=N-1}^{0}\langle\tau|\mathcal{K}_i\mathcal{K}_{i+1}G|\tau\rangle \prod_{i=0}^{N-1}\langle\sigma|\mathcal{J}_{i+1}\mathcal{J}_i G|\sigma\rangle, \tag{4.19}$$

where $\mathcal{J}_0 = \mathcal{K}_0 = I$ and $\mathcal{J}_{i\neq 0} = \mathcal{K}_{i\neq 0} = \left\{I, \bar{X}\right\}$.

### 4.1.3 Normal ordering

Instead of doing the time ordering, we will write the evolution operator in normal order. This will help us advance with our calculation.

We start performing the Magnus expansion (see Section 3.1) of the evolution operator, Eq. (4.13). This expansion is comprised mainly of commutators of the interaction potential. In our case, it stops at second order, since the first commutator is a c-number and not an operator. Applying this procedure, the evolution operator becomes:

$$u(n) = e^{\frac{1}{2}\int_{(n-1)\Delta}^{n\Delta} dt_1 \int_{(n-1)\Delta}^{t_1} dt_2 \left[-i\lambda\sum_{\mathbf{r}} f(\mathbf{r},t_1)\sigma_{\mathbf{r}}^x, -i\lambda\sum_{\mathbf{r}'} f(\mathbf{r}',t_2)\sigma_{\mathbf{s}}^x\right]} e^{-i\lambda\int_{(n-1)\Delta}^{n\Delta} dt\sum_{\mathbf{r}} f(\mathbf{r},t)\sigma_{\mathbf{r}}^x}. \tag{4.20}$$

Then we can use commutation relations to rewrite the last equation's second exponential:

$$\begin{aligned} e^{-i\lambda\int_{(n-1)\Delta}^{n\Delta} dt\sum_{\mathbf{r}} f(\mathbf{r},t)\sigma_{\mathbf{r}}^x} &= e^{-\frac{\lambda^2(v/\omega_0)^{D+2s}}{L^D}\int_{(n-1)\Delta}^{n\Delta} dt\int_{(n-1)\Delta}^{n\Delta} dt_1\sum_{\mathbf{r},\mathbf{r}'}\sum_{\mathbf{k}\neq 0}|\mathbf{k}|^{2s}e^{i\mathbf{k}\cdot(\mathbf{r}-\mathbf{r}')+i\omega_k(t-t_1)}\sigma_{\mathbf{r}}^x\sigma_{\mathbf{r}'}^x} \times \\ &\quad : e^{-i\lambda\int_{(n-1)\Delta}^{n\Delta} dt\sum_{\mathbf{r}} f(\mathbf{r},t)\sigma_{\mathbf{r}}^x} : \end{aligned} \tag{4.21}$$

We can now rearrange the terms and define the Green's functions $\alpha$ and $\mathcal{G}$ to rewrite the evolution operator as:

$$u(k,n) = \prod_k e^{-\mathcal{G}(k,\Delta,0)}e^{-i\alpha(k,n)a_{\mathbf{k}}^{\dagger}}e^{-i\alpha^*(k,n)a_{\mathbf{k}}}, \tag{4.22}$$

where

$$\begin{aligned} \alpha(k,n) &= \frac{\lambda(v/\omega_0)^{D/2+s}}{L^{D/2}}\int_{\Delta(n-1)}^{\Delta n} dt\sum_{\mathbf{r}}|\mathbf{k}|^s\,\sigma_{\mathbf{r},n}^x e^{+i\mathbf{k}\cdot\mathbf{r}+i\omega_k t} \\ &= \frac{2\lambda(v/\omega_0)^{D/2+s}}{L^{D/2}}\sum_{\mathbf{r}}\frac{|\mathbf{k}|^s}{\omega_k}\sigma_{\mathbf{r},n}^x e^{i\mathbf{k}\cdot\mathbf{r}+i\omega_k\Delta\left(n-\frac{1}{2}\right)}\sin\left[\frac{\omega_k\Delta}{2}\right], \end{aligned} \tag{4.23}$$

and

$$\mathcal{G}(k,n) = \frac{\lambda^2 (v/\omega_0)^{D+2s}}{L^D} \int_{\Delta(n-1)}^{\Delta n} dt_1 \int_{\Delta(n-1)}^{t_1} dt_2 \sum_{\mathbf{r},\mathbf{r}'} |\mathbf{k}|^{2s} e^{-i\mathbf{k}\cdot(\mathbf{r}-\mathbf{r}')-i\omega_k(t_1-t_2)} \sigma^x_{\mathbf{r},n}\sigma^x_{\mathbf{r}',n}. \tag{4.24}$$

For the reverse evolution we rename the Green's functions $\alpha \to \beta$, and, as we stated before, we use the spin variable $\sigma \to \tau$ to distinguish the two branches of the Keldysh diagram. So we write:

$$u^\dagger(k,n) = \prod_k e^{-\mathcal{G}^*(k,\Delta,0)} e^{i\beta(k,n)a^\dagger_{\mathbf{k}}} e^{i\beta^*(k,n)a_{\mathbf{k}}}, \tag{4.25}$$

where

$$\beta(k,n) = \frac{\lambda (v/\omega_0)^{D/2+s}}{L^{D/2}} \int_{\Delta(n-1)}^{\Delta n} dt \sum_{\mathbf{r}} |\mathbf{k}|^s \tau^x_{\mathbf{r},n} e^{+i\mathbf{k}\cdot\mathbf{r}+i\omega_k t}. \tag{4.26}$$

We need to normal order the products of evolution operators through quantum error correction cycles. First we have the forward evolution operator:

$$\begin{aligned} u_{N-1}(\sigma)\ldots u_0(\sigma) &= \prod_k e^{-\sum_{i=0}^{N-1}\mathcal{G}(k,i)} e^{-\sum_{n=1}^{N-1}\sum_{m=0}^{n-1}\alpha^*(k,n)\alpha(k,m)} \times \\ & e^{-i\alpha(k,N-1)a^\dagger_{\mathbf{k}}}\ldots e^{-i\alpha(k,0)a^\dagger_{\mathbf{k}}} e^{-i\alpha^*(k,N-1)a_{\mathbf{k}}}\ldots e^{-i\alpha^*(k,0)a_{\mathbf{k}}}, \end{aligned} \tag{4.27}$$

and then the backwards evolution operator:

$$\begin{aligned} u^\dagger_0(\tau)\ldots u^\dagger_{N-1}(\tau) &= \prod_k e^{-\sum_{i=0}^{N-1}\mathcal{G}^*(k,i)} e^{-\sum_{n=0}^{N-1}\beta^*(k,n)\sum_{m=n+1}^{N-1}\beta(k,m)} \times \\ & e^{i\beta(k,N-1)a^\dagger_{\mathbf{k}}}\ldots e^{i\beta(k,0)a^\dagger_{\mathbf{k}}} e^{i\beta^*(k,N-1)a_{\mathbf{k}}}\ldots e^{i\beta^*(k,0)a_{\mathbf{k}}}. \end{aligned} \tag{4.28}$$

Putting the last two equations together and doing the global time ordering, we find that the total evolution operator is:

$$\begin{aligned} & u^\dagger_0(\tau)\ldots u^\dagger_{N-1}(\tau)\, u_{N-1}(\sigma)\ldots u_0(\sigma) = \\ & \prod_k e^{-\sum_{i=0}^{N-1}[\mathcal{G}^*(k,i)+\mathcal{G}(k,i)]} e^{-\sum_{n=0}^{N-1}\sum_{m=n+1}^{N-1}\beta^*(k,n)\beta(k,m)} e^{-\sum_{n=1}^{N-1}\sum_{m=0}^{n-1}\alpha^*(k,n)\alpha(k,m)} e^{\sum_{n=0}^{N-1}\sum_{m=0}^{N-1}\alpha(k,n)\beta^*(k,m)} \times \\ & e^{-i[\alpha(k,N-1)-\beta(k,N-1)]a^\dagger_{\mathbf{k}}}\ldots e^{-i[\alpha(k,0)-\beta(k,0)]a^\dagger_{\mathbf{k}}} e^{-i[\alpha^*(k,N-1)-\beta^*(k,N-1)]a_{\mathbf{k}}}\ldots e^{-i[\alpha*(k,0)-\beta^*(k,0)]a_{\mathbf{k}}} \end{aligned} \tag{4.29}$$

Now we separate the sum over indexes of the same time slice from those of different time slices, i.e.

$$\sum_{n=0}^{N-1}\sum_{m=0}^{N-1} = \sum_{n} + \sum_{n\neq m}, \tag{4.30}$$

where we wrote $\sum_n = \sum_{n=m} = \sum_{n=0}^{N-1}$ and $\sum_{n\neq m} = \sum_{n=0}^{N-1}\sum_{m=0,m\neq n}^{N-1}$. By doing this we get:

$$u_0^\dagger(\tau)\ldots u_{N-1}^\dagger(\tau)\,u_{N-1}(\sigma)\ldots u_0(\sigma) = \prod_k e^{-\sum_n S(\mathbf{k},n)} e^{-\sum_{n\neq m}\mathcal{C}(\mathbf{k},n)} \times e^{-i\sum_n[\alpha(k,n)-\beta(k,n)]a_{\mathbf{k}}^\dagger} e^{-i\sum_n[\alpha^*(k,n)-\beta^*(k,n)]a_{\mathbf{k}}}, \tag{4.31}$$

where

$$S(\mathbf{k},n) = \mathcal{G}^*(k,n) + \mathcal{G}(k,n) - \alpha(k,n)\,\beta^*(k,n) \tag{4.32}$$

is the sum of terms of the same time slice, and

$$\mathcal{C}(\mathbf{k},n) = \alpha^*(k,n)\,\alpha(k,m) + \beta^*(k,n)\,\beta(k,m) - \alpha(k,n)\,\beta^*(k,m) - \alpha(k,m)\,\beta^*(k,n) \tag{4.33}$$

is the sum of terms of different time slices. It is straightforward now to write the expectation value of the vacuum state of the bath:

$$\langle 0|u_0^\dagger(\tau)\ldots u_{N-1}^\dagger(\tau)\,u_{N-1}(\sigma)\ldots u_0(\sigma)\,|0\rangle = \prod_k e^{-\sum_{n=0}^{N-1} S(\mathbf{k},n)} e^{-\sum_n\sum_m \mathcal{C}(\mathbf{k},n)}. \tag{4.34}$$

We need to sum the terms of the same slice $\mathcal{S}(\mathbf{k},n)$ over the bath modes $k$. To that end, we suppose that $\omega_k$ is isotropic in space. In this way we get:

$$\sum_{\mathbf{k}}\mathcal{S}(\mathbf{k}) = \sum_{\mathbf{r},\mathbf{r}'}\left[F(\mathbf{r}-\mathbf{r}')\,(\tau_{\mathbf{r}}^x-\sigma_{\mathbf{r}}^x)\,(\tau_{\mathbf{r}'}^x-\sigma_{\mathbf{r}'}^x) + i\Phi_1(\mathbf{r}-\mathbf{r}')\,(\tau_{\mathbf{r}}^x-\sigma_{\mathbf{r}}^x)\,(\tau_{\mathbf{r}'}^x+\sigma_{\mathbf{r}'}^x)\right] \tag{4.35}$$

And for terms at different time slices, we sum $\mathcal{C}(\mathbf{k},n)$ over the bath modes to get:

$$\sum_{\mathbf{k}\neq 0}\mathcal{C}(\mathbf{k},n) = \sum_{\mathbf{r},\mathbf{r}'}\{[F_c(\mathbf{r}-\mathbf{r}',n-m) - \Phi_{2,s}(\mathbf{r}-\mathbf{r}',n-m)]\,(\tau_{\mathbf{r},n}-\sigma_{\mathbf{r},n})\,(\tau_{\mathbf{r}',m}-\sigma_{\mathbf{r}',m}) + i\,[\Phi_{2,c}(\mathbf{r}-\mathbf{r}',n-m) + F_s(\mathbf{r}-\mathbf{r}',n-m)]\,(\tau_{\mathbf{r},n}-\sigma_{\mathbf{r},n})\,(\tau_{\mathbf{r}',m}+\sigma_{\mathbf{r}',m})\} \tag{4.36}$$

In the last two equations, $F(\mathbf{r}-\mathbf{r}')$, $\Phi_1(\mathbf{r}-\mathbf{r}')$, $\Phi_2(\mathbf{r}-\mathbf{r}')$, $F_c(\mathbf{r}-\mathbf{r}', n-m)$, $\Phi_{2,s}(\mathbf{r}-\mathbf{r}', n-m)$, $\Phi_{2,c}(\mathbf{r}-\mathbf{r}', n-m)$, and $F_s(\mathbf{r}-\mathbf{r}', n-m)$ are all derived from the original Green's functions ($\mathcal{G}(k,n)$, $\alpha(k,n)$, and $\beta(k,n)$). They are also integrated over time and summed over the bath modes. Their expressions are detailed in Appendix B.

Putting all these pieces together and taking the expectation value with the ground state of the bath, we find the following expression for the product of the evolution operators:

$$\langle 0|u_0^\dagger(\tau)\ldots u_{N-1}^\dagger(\tau)\,u_{N-1}(\sigma)\ldots u_0(\sigma)\,|0\rangle = e^{-\mathcal{H}}, \tag{4.37}$$

where

$$\mathcal{H} = \mathcal{H}(\tau,\sigma) = \sum_n \sum_{k\neq 0} \mathcal{S}(\mathbf{k},n) + \sum_{n\neq m} \sum_{k\neq 0} \mathcal{C}(\mathbf{k},n,m)\,. \tag{4.38}$$

Notice that this product looks like a partition function, but it is not as straightforward to calculate since the complete expectation values have the constrains that come from syndrome extraction after each quantum error correction cycle.

### 4.1.4 Fidelity's numerator, and denominator

Returning to the original problem, we proceed to examine the two expectation values involved in the fidelity. Its numerator (Equation (4.18)), which we can now write as:

$$\langle\psi|\left(|\bar{\uparrow}\rangle\langle\bar{\uparrow}|\right)|\psi\rangle = \sum_{S,Q}\sum_{\mathcal{K}\mathcal{J}} e^{-\mathcal{H}} \prod_{i=0}^{N-1} \langle\tau|\mathcal{K}_i\mathcal{K}_{i+1}G|\tau\rangle \prod_{j=N-1}^{0} \langle\sigma|\mathcal{J}_{j+1}\mathcal{J}_j G|\sigma\rangle, \tag{4.39}$$

where $\mathcal{J}_0 = \mathcal{K}_0 = \mathcal{J}_N = \mathcal{K}_N = I$, and $\mathcal{J}_{i\neq 0,N} = \mathcal{K}_{i\neq 0,N} = \left\{I, \bar{X}\right\}$, as before. And its denominator (Equation (4.19)), which takes the same form:

$$\langle\psi|\psi\rangle = \sum_{S,Q}\sum_{\mathcal{K}\mathcal{J}} e^{-\mathcal{H}} \prod_{i=0}^{N-1} \langle\tau|\mathcal{K}_i\mathcal{K}_{i+1}G|\tau\rangle \prod_{j=N-1}^{0} \langle\sigma|\mathcal{J}_{j+1}\mathcal{J}_j G|\sigma\rangle, \tag{4.40}$$

but with different restrictions, namely $\mathcal{J}_0 = \mathcal{K}_0 = I$, $\mathcal{K}_N = \mathcal{J}_N$, and $\mathcal{J}_{i\neq 0} = \mathcal{K}_{i\neq 0} = \left\{I, \bar{X}\right\}$.

Until now everything has been done exactly, but to be able to get some results we need to make simplifications. The first one is that if $\omega_k$ is isotropic, then both $\Phi_{2,c}(\mathbf{r},n)$, and $F_s(\mathbf{r},n)$ go to zero because we are integrating odd functions over all $\mathbf{k}$ (see Appendix B). Then we can

rewrite $\mathcal{H}$ as:

$$\mathcal{H} = \sum_{\mathbf{r},\mathbf{r}'} \left\{ \sum_{n \neq m} \left[ F_c \left( \mathbf{r} - \mathbf{r}', n - m \right) - \Phi_{2,s} \left( \mathbf{r} - \mathbf{r}', n - m \right) \right] \left( \tau_{\mathbf{r},n} - \sigma_{\mathbf{r},n} \right) \left( \tau_{\mathbf{r}',m} - \sigma_{\mathbf{r}',m} \right) \right.$$
$$\left. + \left[ F \left( \mathbf{r} - \mathbf{r}' \right) \sum_n \left( \tau_{\mathbf{r},n} - \sigma_{\mathbf{r},n} \right) \left( \tau_{\mathbf{r}',n} - \sigma_{\mathbf{r}',n} \right) + i \Phi_1 \left( \mathbf{r} - \mathbf{r}' \right) \sum_n \left( \tau_{\mathbf{r},n} - \sigma_{\mathbf{r},n} \right) \left( \tau_{\mathbf{r}',n} + \sigma_{\mathbf{r}',n} \right) \right] \right\} \tag{4.41}$$

It is also useful to separate the sum with $\mathbf{r} = \mathbf{r}'$, and the rest. Since $\Phi_{2,s}(0,n) = 0$ (Appendix B), $\mathcal{H}$ becomes:

$$\mathcal{H} = \sum_{\mathbf{r}} \left\{ \sum_{n \neq m} F_c \left( 0, n - m \right) \left( \tau_{\mathbf{r},n} - \sigma_{\mathbf{r},n} \right) \left( \tau_{\mathbf{r},m} - \sigma_{\mathbf{r},m} \right) \right.$$
$$\left. + \left[ F \left( 0 \right) \sum_n \left( \tau_{\mathbf{r},n} - \sigma_{\mathbf{r},n} \right) \left( \tau_{\mathbf{r}',n} - \sigma_{\mathbf{r}',n} \right) + i \Phi_1 \left( 0 \right) \sum_n \left( \tau_{\mathbf{r},n} - \sigma_{\mathbf{r},n} \right) \left( \tau_{\mathbf{r},n} + \sigma_{\mathbf{r},n} \right) \right] \right\}$$
$$+ \sum_{\mathbf{r} \neq \mathbf{r}'} \left\{ \sum_{n \neq m} \left[ F_c \left( \mathbf{r} - \mathbf{r}', n - m \right) - \Phi_{2,s} \left( \mathbf{r} - \mathbf{r}', n - m \right) \right] \left( \tau_{\mathbf{r},n} - \sigma_{\mathbf{r},n} \right) \left( \tau_{\mathbf{r}',m} - \sigma_{\mathbf{r}',m} \right) \right.$$
$$\left. + \left[ F \left( \mathbf{r} - \mathbf{r}' \right) \sum_n \left( \tau_{\mathbf{r},n} - \sigma_{\mathbf{r},n} \right) \left( \tau_{\mathbf{r}',n} - \sigma_{\mathbf{r}',n} \right) + i \Phi_1 \left( \mathbf{r} - \mathbf{r}' \right) \sum_n \left( \tau_{\mathbf{r},n} - \sigma_{\mathbf{r},n} \right) \left( \tau_{\mathbf{r}',n} + \sigma_{\mathbf{r}',n} \right) \right] \right\} \tag{4.42}$$

We separate now the real and imaginary parts and use the fact that

$$\sin \left[ \sum_n \sum_{\mathbf{r} \neq \mathbf{r}'} \Phi_1 \left( \mathbf{r} - \mathbf{r}' \right) \left( \tau_{\mathbf{r},n} - \sigma_{\mathbf{r},n} \right) \left( \tau_{\mathbf{r}',n} + \sigma_{\mathbf{r}',n} \right) \right] = 0,$$

so that the expectation value in the numerator of the fidelity can be written as:

$$\langle \psi | \left( |\bar{\uparrow}\rangle\langle\bar{\uparrow}| \right) |\psi\rangle = \sum_{S,Q} \sum_{\mathcal{K}\mathcal{J}} e^{-\mathcal{H}} \cos \left[ \Phi_1 \left( 0 \right) \sum_n \sum_{\mathbf{r}} \left( \tau_{\mathbf{r},n} - \sigma_{\mathbf{r},n} \right) \left( \tau_{\mathbf{r},n} + \sigma_{\mathbf{r},n} \right) \right] \times$$
$$\cos \left[ \sum_n \sum_{\mathbf{r} \neq \mathbf{r}'} \Phi_1 \left( \mathbf{r} - \mathbf{r}' \right) \left( \tau_{\mathbf{r},n} - \sigma_{\mathbf{r},n} \right) \left( \tau_{\mathbf{r}',n} + \sigma_{\mathbf{r}',n} \right) \right] \prod_{i=0}^{N-1} \langle \tau | \mathcal{K}_i \mathcal{K}_{i+1} G | \tau \rangle \prod_{j=N-1}^{0} \langle \sigma | \mathcal{J}_{j+1} \mathcal{J}_j G | \sigma \rangle \tag{4.43}$$

with $\mathcal{K}_i$, and $\mathcal{J}_i$ again following the prescriptions we gave before (Equation (4.15)), and

$$\mathcal{H} = \sum_{\mathbf{r}} F(\mathbf{r}-\mathbf{r}') \sum_{n} (\tau_{\mathbf{r},n} - \sigma_{\mathbf{r},n})(\tau_{\mathbf{r}',n} - \sigma_{\mathbf{r}',n}) + \sum_{n\neq m}\sum_{\mathbf{r}} F_c(0, n-m)(\tau_{\mathbf{r},n} - \sigma_{\mathbf{r},n})(\tau_{\mathbf{r},m} - \sigma_{\mathbf{r},m})$$
$$+ \sum_{n\neq m}\sum_{\mathbf{r}\neq\mathbf{r}'} [F_c(\mathbf{r}-\mathbf{r}', n-m) - \Phi_{2,s}(\mathbf{r}-\mathbf{r}', n-m)](\tau_{\mathbf{r},n} - \sigma_{\mathbf{r},n})(\tau_{\mathbf{r}',m} - \sigma_{\mathbf{r}',m}). \quad (4.44)$$

Also note that the expectation value in the denominator has the same form, with prescriptions for $\mathcal{K}_i$, and $\mathcal{J}_i$ specified in Equation (4.16).

Now we will separate the term $n = m$:

$$\mathcal{H} = F_c(0,0)\sum_{n}\sum_{\mathbf{r}} (\tau_{\mathbf{r},n} - \sigma_{\mathbf{r},n})(\tau_{\mathbf{r},n} - \sigma_{\mathbf{r},n})$$
$$+\sum_{\mathbf{r}\neq\mathbf{r}'}\sum_{n} F_c(\mathbf{r}-\mathbf{r}', 0)(\tau_{\mathbf{r},n} - \sigma_{\mathbf{r},n})(\tau_{\mathbf{r}',n} - \sigma_{\mathbf{r}',n}) + \sum_{n\neq m}\sum_{\mathbf{r}} F_c(0, n-m)(\tau_{\mathbf{r},n} - \sigma_{\mathbf{r},n})(\tau_{\mathbf{r},m} - \sigma_{\mathbf{r},m})$$
$$+ \sum_{n\neq m}\sum_{\mathbf{r}\neq\mathbf{r}'} [F_c(\mathbf{r}-\mathbf{r}', n-m) - \Phi_{2,s}(\mathbf{r}-\mathbf{r}', n-m)](\tau_{\mathbf{r},n} - \sigma_{\mathbf{r},n})(\tau_{\mathbf{r}',m} - \sigma_{\mathbf{r}',m}). \quad (4.45)$$

We took into account that $\Phi_{2,s}(\mathbf{r}, 0) = \frac{\lambda^2}{L^D}\sum_{\mathbf{k}\neq 0} |\mathbf{k}|^{2s} \sin(\mathbf{k}\cdot\mathbf{r}) \sin(0) \frac{1-\cos[\omega_k \Delta]}{\omega_k^2} = 0$, $F(\mathbf{r}-\mathbf{r}') = F_c(\mathbf{r}-\mathbf{r}', 0)$, and that $F(0) = F_c(0,0)$ (details of this in Appendix B).

One more simplification can be done. Notice that the sum over space and time of the spin variables in the first cosine adds up to zero:

$$\sum_{n=0}^{N-1}\sum_{\mathbf{r}} (\tau_{\mathbf{r},n} - \sigma_{\mathbf{r},n})(\tau_{\mathbf{r},n} + \sigma_{\mathbf{r},n}) = \sum_{n=0}^{N-1}\sum_{\mathbf{r}} (\tau_{\mathbf{r},n}\tau_{\mathbf{r},n} - \sigma_{\mathbf{r},n}\sigma_{\mathbf{r},n}) = N_s N - N_s N = 0. \quad (4.46)$$

Then the expectation value in the numerator is:

$$\langle\psi|\left(|\bar{\uparrow}\rangle\langle\bar{\uparrow}|\right)|\psi\rangle = \sum_{S,Q}\sum_{\mathcal{K}\mathcal{J}} e^{-\mathcal{H}} \cos\left[\sum_{n}\sum_{\mathbf{r}\neq\mathbf{r}'} \Phi_1(\mathbf{r}-\mathbf{r}')(\tau_{\mathbf{r},n} - \sigma_{\mathbf{r},n})(\tau_{\mathbf{r}',n} + \sigma_{\mathbf{r}',n})\right] \times$$
$$\prod_{i=0}^{N-1} \langle\tau|\mathcal{K}_i\mathcal{K}_{i+1}G|\tau\rangle \prod_{j=N-1}^{0} \langle\sigma|\mathcal{J}_{j+1}\mathcal{J}_j G|\sigma\rangle \quad (4.47)$$

with

$$\mathcal{H} = F_c(0,0)\sum_n\sum_{\mathbf{r}}(\tau_{\mathbf{r},n}-\sigma_{\mathbf{r},n})(\tau_{\mathbf{r},n}-\sigma_{\mathbf{r},n})$$
$$+\sum_n\sum_{\mathbf{r}\neq\mathbf{r}'}F_c(\mathbf{r}-\mathbf{r}',0)(\tau_{\mathbf{r},n}-\sigma_{\mathbf{r},n})(\tau_{\mathbf{r}',n}-\sigma_{\mathbf{r}',n})+\sum_{n\neq m}\sum_{\mathbf{r}}F_c(0,n-m)(\tau_{\mathbf{r},n}-\sigma_{\mathbf{r},n})(\tau_{\mathbf{r},m}-\sigma_{\mathbf{r},m})$$
$$+\sum_{n\neq m}\sum_{\mathbf{r}\neq\mathbf{r}'}[F_c(\mathbf{r}-\mathbf{r}',n-m)-\Phi_{2,s}(\mathbf{r}-\mathbf{r}',n-m)](\tau_{\mathbf{r},n}-\sigma_{\mathbf{r},n})(\tau_{\mathbf{r}',m}-\sigma_{\mathbf{r}',m}), \quad (4.48)$$

and the restrictions we already stated for $\mathcal{K}$, and $\mathcal{J}$ (Equation (4.15)).

## 4.2 Super-ohmic dissipation

From now on we investigate the super-ohmic regime. This special case has the property that correlations decay very rapidly through spatial dimensions. In particular, we show in Appendix B that, for $s = 1/2$, the ratio of coupling constants to first neighbors to the coupling constants that come from self-interactions goes to zero as the high-frequency cut-off $\Lambda^2$ of the bath diverges:

$$\frac{F_c(z,0)}{F_c(0,0)} \sim \frac{F_c(z,1)}{F_c(0,0)} \sim \frac{F_c(z,0)}{F_c(0,1)} \sim \frac{F_c(z,1)}{F_c(0,1)} \sim \frac{1}{\Lambda} \quad (4.49)$$

and

$$\frac{\Phi_1(z)}{F_c(0,0)} \sim \frac{\Phi_1(z)}{F_c(0,1)} \sim \frac{1}{\Lambda^{1/2}}, \quad (4.50)$$

where $z = a/v\Delta$ is a dimensionless parameter which involves the lattice constant $a$, the propagation velocity of excitations $v$, and the quantum error correction period $\Delta$.

Doing this approximation, our exponent becomes:

$$\mathcal{H} \approx F_c(0,0)\sum_{n=0}^{N-1}(\tau_{\mathbf{r},n}-\sigma_{\mathbf{r},n})(\tau_{\mathbf{r},n}-\sigma_{\mathbf{r},n})+\sum_{n\neq m}\sum_{\mathbf{r}}F_c(0,n-m)(\tau_{\mathbf{r},n}-\sigma_{\mathbf{r},n})(\tau_{\mathbf{r},m}-\sigma_{\mathbf{r},m}). \quad (4.51)$$

This approximation simplifies greatly our problem because we can restrict our attention only to auto-correlations and, at the same time, lets us make a correspondence of our phenomenological model with a concrete type of environment.

[2] $\Lambda$ is the highest frequency the bosonic modes of the bath have. It appears when we take the continuum limit and integrate: $\sum_k \to \frac{(2\pi)^2}{L^2}\sum_{\mathbf{k}} \to \int d^2k = \int_0^\Lambda kdk\int_0^{2\pi}d\theta$.

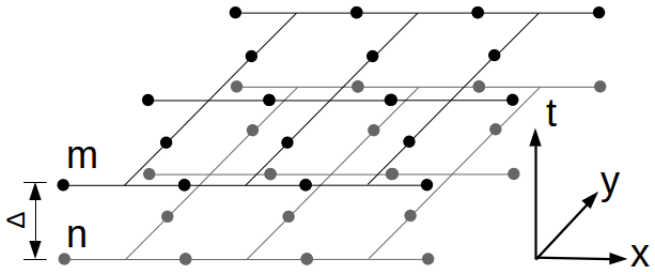


Figure 4.2: Equivalent spin lattice: each 2D slice corresponds to the time of each syndrome extraction, time runs in the vertical axis.

### 4.2.1 Error threshold as a phase transition

In this Section we return to the ideas we presented in Section 3.5, which suggests us that the error threshold can be thought of as a quantum phase transition. To accomplish this we identify a parameter in the bath that we can vary, and find two different regimes. In one of them the fidelity has value one (successful error correction), and another in which the fidelity decays to small values (loss of information): these regimes correspond to two phases of a statistical model analog (Figure 4.2) to our quantum computer with dissipation. Then the critical value of this parameter, would determine the error threshold.

To find this critical behavior, it is convenient to start by rewriting the fidelity, Equation (4.3), in terms of two quantities $\mathcal{A}$, and $\mathcal{B}$ as:

$$\mathcal{F} = \frac{\langle\psi|\left(|\bar{\uparrow}\rangle\langle\bar{\uparrow}|\right)|\psi\rangle}{\langle\psi|\psi\rangle} = \frac{\mathcal{A}}{\mathcal{A}+\mathcal{B}}. \tag{4.52}$$

What we gain here is that the behavior of the fidelity will depend on $\mathcal{B}$. When $\mathcal{B} = 0$ the fidelity has value $1$, and for $\mathcal{B} \neq 0$ the fidelity will always be less than $1$. Thus from now on we can restrict our attention to this new function $\mathcal{B}$.

To find an expression for $\mathcal{B}$, we first note that trivially that $\mathcal{A} = \langle\psi|\bar{\uparrow}\rangle\langle\bar{\uparrow}|\psi\rangle$. Then, after some manipulation detailed in Appendix A.3, we get the expression:

$$\begin{aligned}\mathcal{B} &= \langle\psi|\psi\rangle - \mathcal{A} \\ &= \sum_{\sigma,\tau}{\sum_{\{\mathcal{K}\},\{\mathcal{J}\}}}'' e^{-\mathcal{H}} \prod_{i=0}^{N-1} \langle\tau|\mathcal{K}_i\mathcal{K}_{i+1}G|\tau\rangle \prod_{j=N-1}^{0} \langle\sigma|\mathcal{J}_{j+1}\mathcal{J}_j G|\sigma\rangle,\end{aligned} \tag{4.53}$$

where the sum $\sum''$ has the restrictions $\mathcal{J}_0 = \mathcal{K}_0 = I$, $\mathcal{J}_N = \mathcal{K}_N = \bar{X}$, and $\mathcal{J}_{i\neq 0,N} = \mathcal{K}_{i\neq 0,N} = \{I, \bar{X}\}$. Notice that $\mathcal{B}$ has the form of a partition function, with $\mathcal{H}$ being the Hamiltonian, but it has the positive plaquette restrictions due to the projection operators at the end of each

error correction cycle.

### 4.2.2 Physical meaning of the restrictions in the expectation values

We are going to expand the sum $\sum''_{\{\mathcal{K}\},\{\mathcal{J}\}}$, which involves mainly the factors $\langle\tau|\mathcal{K}_i\mathcal{K}_{i+1}G|\tau\rangle$ and $\langle\sigma|\mathcal{J}_{i+1}\mathcal{J}_iG|\sigma\rangle$.

Firstly we will see that, due to the presence of the projection operators, if the initial state of our memory is in the logical up (down) state, the form of the projector forces it to propagate through time.

We can show this in the following manner. Let us look at the product

$$\dots PUPU|\psi_0\rangle, \tag{4.54}$$

where the projection operator in the basis of the logical qubit is:

$$P = |\bar{\uparrow}\rangle\langle\bar{\uparrow}| + \bar{X}|\bar{\uparrow}\rangle\langle\bar{\uparrow}|\bar{X} = |\bar{\uparrow}\rangle\langle\bar{\uparrow}| + |\bar{\downarrow}\rangle\langle\bar{\downarrow}| \tag{4.55}$$

So, if $|\psi_0\rangle = |\bar{\uparrow}\rangle$:

$$PU|\psi_0\rangle \propto P|\bar{\uparrow}\rangle = |\bar{\uparrow}\rangle\langle\bar{\uparrow}|\bar{\uparrow}\rangle, \tag{4.56}$$

and if $|\psi_0\rangle = |\bar{\downarrow}\rangle = \bar{X}|\bar{\uparrow}\rangle$:

$$PU|\psi_0\rangle \propto P|\bar{\downarrow}\rangle = |\bar{\downarrow}\rangle\langle\bar{\downarrow}|\bar{\downarrow}\rangle. \tag{4.57}$$

We will use this fact to write a simplified version of the restrictions. But first we need to remember that since we are working in the $x$ basis, then instead of up and down states we use $+$ and $-$ states (see Equation (4.17)). Those states are related by a $\bar{Z}$ operator. For the $\sigma$ variables we write $\left\{|\sigma_i^+\rangle\right\}$, and $\left\{|\sigma_i^-\rangle\right\}$, where:

$$|\sigma_i^+\rangle = \prod_j B_{\square_j}|F_x\rangle_i, \text{ and } |\sigma_i^-\rangle = \bar{Z}_i^\gamma|\sigma_i^+\rangle. \tag{4.58}$$

Then the restrictions in this basis are:

$$\langle\sigma_i^+|\bar{X}G|\sigma_i^+\rangle = +\langle\sigma_i^+|G|\sigma_i^+\rangle, \tag{4.59}$$

and

$$\langle\sigma_i^-|\bar{X}G|\sigma_i^-\rangle = \langle\sigma_i^+|\bar{Z}\bar{X}\bar{Z}G|\sigma_i^+\rangle = -\langle\sigma_i^-|G|\sigma_i^-\rangle. \tag{4.60}$$

In the last line we used the fact that $\bar{Z}$ anti-commutes with $\bar{X}$, and $\bar{Z}\bar{Z} = 1$.

We will use the shorthand notation $\langle\sigma_i^\alpha|G|\sigma_i^\alpha\rangle = G\left(\sigma_i^\alpha\right)$, where $\alpha = +, -$. Notice that the $\tau$ variable follows the same structure.

Then, using this notation and the fact that the form of the initial state propagates through quantum error correction cycles, $\mathcal{B}$ has can be written as:

$$\mathcal{B} \approx \sum_{\sigma,\tau} e^{-\mathcal{H}} \prod_{i=0}^{N-1}\prod_{j=0}^{N-1} \left[G\left(\tau_i^+\right)G\left(\sigma_j^+\right) + G\left(\tau_i^-\right)G\left(\sigma_j^-\right) - G\left(\tau_i^+\right)G\left(\sigma_j^-\right) - G\left(\tau_i^-\right)G\left(\sigma_j^+\right)\right], \tag{4.61}$$

where we use the approximate sign because of all the assumptions we have made until here.

### 4.2.3 $S = 1$ Ising chain

For some insight in the time structure of our model, we notice that although we have restrictions $G\left(\tau_i^\pm\right)$ and $G\left(\sigma_j^\pm\right)$ for each of the time slices, the couplings on the vertical (time) axis are free of restrictions. Then, by making the change of variables:

$$S_{\mathbf{r},m} = \tau_{\mathbf{r},m} - \sigma_{\mathbf{r},m}, \tag{4.62}$$

we see that our Hamilitonian $\mathcal{H}$ is analogous to a collection of spin $1$ chains with couplings in the time direction:

$$\mathcal{H} = \sum_{\mathbf{r}} \mathcal{H}_{\mathbf{r}} = \sum_{\mathbf{r}} \left( D\sum_{n=0}^{N-1} S_{\mathbf{r},n}^2 - J\sum_{\langle n,m\rangle} S_{\mathbf{r},n}S_{\mathbf{r},m} \right), \tag{4.63}$$

where

$$\mathcal{H}_{\mathbf{r}} = D\sum_{n=0}^{N-1} S_{\mathbf{r},n}^2 - J\sum_{\langle n,m\rangle} S_{\mathbf{r},n}S_{\mathbf{r},m},$$

$D = \frac{5}{4}F_c(0,0)$, and $J = -F_c(0,1)$.

Capel [44] studied a similar Hamiltonian:

$$\mathcal{H} = -D\sum_i \left(1 - S_{zi}^2\right) - J\sum_{\langle i,j\rangle} S_{zi}S_{zj} - \mu H\sum_i S_{zi}, \tag{4.64}$$

where $D$ is "zero-field splitting, i.e. the separation between singlet and doublet", and $J$ is the exchange parameter.

Our model only differ from Capel's in that our model has no external magnetic field, and lacks the constant $-D\sum_i 1 = -DN$, where $N$ is the number of spins. But Capel studies the case with no magnetic field, and the constant $DN$ does not intervene in the dynamics.

Then the important result for us is that for $H = 0$, there is no magnetic order for $D > \frac{1}{2}zJ$ ($z$ is the number of nearest neighbors).

In Appendix B, we evaluated $F_c(0,0)$ and $F(0,1)$ for $2s - 1 = 0$ or $s = 1/2$. Then, we know that:

$$F_c(0,0) \approx \frac{\lambda^2 v}{2\pi\omega_0^3}\Lambda, \tag{4.65}$$

and

$$F_c(z=0,1) \approx -\frac{\lambda^2 v}{2\pi\omega_0^3}\frac{\Lambda}{2}, \tag{4.66}$$

so that $F_c(0,1) = -\frac{F_c(0,0)}{2}$. From this relation, and since $D = F_c(0,0)$, and $J = -F_c(0,1)$ we get $J = \frac{1}{2}D$. This implies that $D > J$, which means that our model does not present phase transitions and it will remain in its disordered phase.

What we need to remember is that we have the restrictions $G\left(\tau_i^+\right)$, $\bar{G}\left(\tau_i^+\right)$, etc., which constrain the possible configurations inside each of the time slices. This makes so that we can have order in each of the slices, although there is no order in the time direction. Then we need only to solve a 2D problem to find the critical temperature.

For this reasons we now only need to study the expression:

$$\mathcal{B}' \approx \sum_{\sigma,\tau} e^{-\mathcal{H}_1} \left[ G\left(\tau^+\right) G\left(\sigma^+\right) + G\left(\tau^-\right) G\left(\sigma^-\right) - G\left(\tau^+\right) G\left(\sigma^-\right) - G\left(\tau^-\right) G\left(\sigma^+\right) \right], \tag{4.67}$$

with $\mathcal{H}_1 = F_c\left(0,0\right) \sum_{\mathbf{r}} \left(\tau_{\mathbf{r}} - \sigma_{\mathbf{r}}\right)^2$. Notice that this model has the same critical temperature as Eq. (4.61).

### 4.2.4 Critical temperature

Let us rewrite the Hamiltonian $\mathcal{H}_1$ of our equivalent model:

$$\mathcal{H}_1 = F_c\left(0,0\right) \left( N_s - \sum_{\mathbf{r}} \tau_{\mathbf{r}} \sigma_{\mathbf{r}} \right), \tag{4.68}$$

here $N_s$ is the number of spins. Now we can define the mass fields $\mu$ for $\sigma$, and $\nu$ for $\tau$. Mass fields are variables located at the center of each plaquette [17]. They take the values $+1$ or $-1$, and they are arranged so that any spin inside the surface code can be written as the product of its two nearest mass fields. For example, in Fig. 4.3,

$$\sigma_{\mathbf{r}} = \mu_{\mathbf{x}} \mu_{\mathbf{y}}. \tag{4.69}$$

Notice that the same structure is valid for the $\tau$ variable, i.e. $\tau_{\mathbf{r}} = \nu_{\mathbf{x}} \nu_{\mathbf{y}}$.

Mass fields are useful for us because, in writing our Hamiltonian in terms of them, the restrictions for positive stars are automatically met. This can be easily seen: the mass fields appearing in a star operator $A_S$ repeat themselves twice from the product of adjacent spin variables. Since, for any $\mathbf{x}$ we have $\mu_{\mathbf{x}} = \pm 1$, then $\mu_{\mathbf{x}} \mu_{\mathbf{x}} = 1$, and thus $A_S = 1$ for all lattice positions.

Nevertheless, at the top and bottom boundaries of our lattice we have a complication: stars located there are formed by only three qubits, and moreover qubits at those boundaries have only one adjacent mass field. In the Figure 4.3, we have the example of the operator $A_S = \sigma_{\mathbf{r}'} \sigma_{\mathbf{r}''} \sigma_{\mathbf{r}'''}$.

Let us start studying this situation by noticing that $\sigma_{\mathbf{r}'''} = \mu_{\mathbf{x}'} \mu_{\mathbf{x}''}$, because the qubit at $\mathbf{r}'''$ is in the bulk. And since all star operators must have positive eigenvalues, $A_S = \sigma_{\mathbf{r}'} \sigma_{\mathbf{r}''} \sigma_{\mathbf{r}'''} = 1$. Using this two equations we get $\mu_{\mathbf{x}'} \mu_{\mathbf{x}''} \sigma_{\mathbf{r}'} \sigma_{\mathbf{r}''} = 1$. Now we multiply $\mu_{\mathbf{x}''} \sigma_{\mathbf{r}''}$ at both sides of last equation to get:

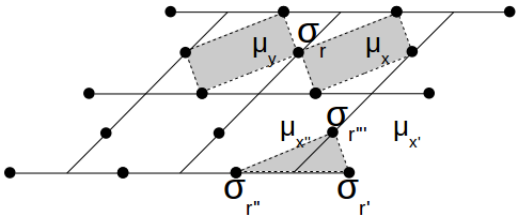


Figure 4.3: Example of mass fields in the bulk, and in the boundary for the $\sigma$ variable.

$$\mu_{\mathbf{x}'}\sigma_{\mathbf{r}'} = \mu_{\mathbf{x}''}\sigma_{\mathbf{r}''} := \alpha, \tag{4.70}$$

where $\alpha$ is a constant with value $+1$ or $-1$. We can follow the same procedure with all spins at each boundary. Although the constant $\alpha$ we defined can assume two values it has to be the same for all spins at one boundary.

Using Equations (4.69), and (4.70), we get:

$$\mathcal{H}_1 = F_c\left(0,0\right)\left(N_s - \sum_{\langle \mathbf{x},\mathbf{y}\rangle \in \text{bulk}} \nu_{\mathbf{x}}\nu_{\mathbf{y}}\mu_{\mathbf{x}}\mu_{\mathbf{y}} - \sum_{\mathbf{x}\in\text{bound}} \alpha_{\mathbf{x}}\nu_{\mathbf{x}}\mu_{\mathbf{x}}\right), \tag{4.71}$$

which still appears to have a complicated form.

Finally, we define a new spin variable $s_{\mathbf{r}} = \nu_{\mathbf{r}}\mu_{\mathbf{r}}$, $s_{\mathbf{r}} = \pm 1$. Then our equivalent Hamiltonian has a more familiar form:

$$\mathcal{H}_1 = F_c\left(0,0\right)\left(N_s - \sum_{\langle \mathbf{x},\mathbf{y}\rangle \in \text{bulk}} s_{\mathbf{x}}s_{\mathbf{y}} - \sum_{\mathbf{x}\in\text{bound}} \alpha_{\mathbf{x}}s_{\mathbf{x}}\right). \tag{4.72}$$

This is now simply an Ising model with a magnetic field at the boundary. This model without a boundary magnetic field, was first studied by Onsager [45]. The boundary magnetic fields do not affect the phase transition value of the model, and then the transition temperature of the system corresponds to the bulk's temperature. Then the critical temperature is such that:

$$\frac{1}{\beta_c J} = \frac{2}{\ln\left(1+\sqrt{2}\right)} \approx 2,26918531421. \tag{4.73}$$

From Equation (4.72), we know that $\beta_c J = F_c\left(0,0\right)$ and, as we show in Appendix B, $F_c\left(0,0\right) \approx \lambda^2\Lambda v/2\pi\omega_0^3$. This leads to two important results.

Firstly, using these relations and Equation (4.73), we obtain the threshold condition:

$$\frac{2\pi\omega_0^3}{\Lambda v}\frac{1}{(\lambda_c)^2} = \frac{2}{\ln\left(1+\sqrt{2}\right)} \implies \lambda_c = \sqrt{\frac{\pi\omega_0^3 \ln\left(1+\sqrt{2}\right)}{v\Lambda}}, \tag{4.74}$$

where $\lambda_c$ corresponds to the critical (or threshold) value of the coupling constant. This is the equivalent of the accuracy threshold for our model. Then for couplings below $\lambda_c$ the quantum information can be stored reliably and for couplings larger than $\lambda_c$ the contrary is true.

Secondly, we can use these equations and the fact that $\beta_c = 1/kT_c$ to relate the coupling constant of the original model to the temperature of the equivalent model:

$$T_c \propto 1/\left(\lambda_c\right)^2. \tag{4.75}$$

This relation lets us identify the phases of the model to the error correction regimes. The disordered phase of the spin system corresponds to $T > T_c$ and thus to $\lambda < \lambda_c$ which is the regime in which quantum information can be stored reliably. The ordered phase of the equivalent spin system ($T < T_c$) then corresponds to the regime in which quantum information is lost due to the effect of the environment ($\lambda > \lambda_c$).

# Chapter 5

# Conclusions

Our analysis was centered around the threshold theorem, an important result of quantum error correction theory. The threshold theorem's validity is fundamental in order to guarantee the possibility of future implementation of quantum computers that can solve meaningful problems.

In order to study more adequately the interaction between the quantum computer and its environment, we went beyond the traditional approach used in quantum error correction theory, which employs stochastic error models.

The phenomenological model we used for the environment can account for correlations, memory effects, and variable coupling strength of the environment with the system of interest.

With all this in mind, we studied the time evolution of a quantum memory to which its performed quantum error correction periodically using the surface code. We followed the approach that Novais, Mucciolo and collaborators have developed. But, while they investigated the time evolution for one error correction cycle, here we considered $N$ quantum error correction cycles and we specifically solved the case of super-ohmic dissipation.

This dynamical problem was mapped onto an statistical mechanical one, similarly to what has been done in previous works. We established that, for the super-ohmic dissipation regime, ~~this~~ the equivalent spin model is such that even the first-neighbors' couplings (i.e. proportional to $\sigma_{\mathbf{r},n}\sigma_{\mathbf{r}\pm\mathbf{a},n}$ or $\sigma_{\mathbf{r},n}\sigma_{\mathbf{r},n\pm1}$) are negligible in comparison to the on-site (proportional to $\sigma_{\mathbf{r},n}\sigma_{\mathbf{r},n}$) contributions to the Hamiltonian.

Because of this locality, the critical behavior of our model is defined by the positive star restriction enforced by the projection operators inside each of the horizontal planes, and not due to couplings between spins in the vertical (time) direction. This leads us to conclude that,

for the super-ohmic case, (1) one or many error correction cycles lead to the same value of the accuracy threshold, and that (2) our environment does not have memory and its effect is equivalent to that of an stochastic model.

The threshold value for the coupling constant $\lambda^*$ was found be inversely proportional to the ultra-violet cutoff $\Lambda$ of the environment and to the propagation velocity of the excitations $v$.

Also, we found that the temperature of the equivalent spin model is inversely proportional to the coupling constant of the original model, $T \propto \lambda^{-2}$. Thus $\lambda < \lambda^*$ corresponds to the regime were quantum information can be stored reliably and to the disordered phase of the equivalent spin system, and $\lambda > \lambda^*$ corresponds to the regime were quantum information is lost to the environment and to the ordered phase of the equivalent model.

Our work can be continued in various directions. Correlations in the Ohmic and sub-Ohmic regimes make them more difficult to tackle, but nonetheless it is very important to study them in order to characterize completely the threshold theorem for a quantum memory coupled to a correlated environment.

What we can state for sure about those two regimes is that the contribution of the couplings between different spins in the equivalent model will become relevant. Actually we could not ~~from~~ obtain information about the threshold for this regimes because the integrals involved in calculating the coupling constants are very convoluted to calculate analytically and sometimes they even diverge.

Also the value of the threshold is probably only going to decrease, since correlation between qubits is likely to accelerate the decoherence process and it may lead to a greater probability of high-order errors (long chains of $\sigma^x$ operators in our case).

Numerical calculations were also outside the scope of this work. They would help find concrete values for the threshold and establish probabilities of errors where the scaling dimension allows it.

Our results could also be applied to realistic systems that could be or are implemented in the laboratory. Since the final goal is to implement a quantum computer, this is a very desirable objective for the near future.

# Bibliography

[1] Charles H. Bennett. Notes on Landauer's principle, reversible computation, and Maxwell's Demon. *Studies in History and Philosophy of Modern Physics*, 34:501–510, 2003. 10

[2] Steven B. Giddings. Black holes, quantum information, and the foundations of physics. *Physics Today*, 66(4):30, 2013. 10

[3] M. A. Nielsen and I. L. Chuang. *Quantum Computation and Quantum Information*. Cambridge University Press, Cambridge UK, 2000. 10, 11, 12, 17, 19, 22, 24, 28, 31, 32, 38, 40, 44, 45, 54

[4] Richard P. Feynman. Simulating Physics with Computers. *International Journal of Theoretical Physcis*, 21(6/7):467 – 488, 1982. 10

[5] David P. DiVincenzo. Fault-tolerant architectures for superconducting qubits. *Phys. Scr.*, T137:014020, 2009. 11

[6] S. Debnath, N. M. Linke, C. Figgatt, K. A. Landsman, K. Wright, and C. Monroe. Demonstration of a small programmable quantum computer with atomic qubits. *Nature*, 536:63–66, 4 August 2016. 11

[7] Mustafa Ahmed Ali Ahmed, Gonzalo A. Álvarez, and Dieter Suter. Robustness of dynamical decoupling sequences. *Physical Review A*, 87:042309, 2013. 11

[8] Andrea Crespi, Roberto Osellame, Roberta Ramponi, Vittorio Giovannetti, Rosario Fazio, Linda Sansoni, Francesco De Nicola, Fabio Sciarrino, and Paolo Mataloni. Anderson localization of entangled photons in an integrated quantum walk. *Nature Photonics*, 7:322–328, 3 April 2013. 11

[9] Troels F. Ronnow, Zhihui Wang, Joshua Job, Sergio Boixo, Sergei V. Isakov, David Wecker, John M. Martinis, Daniel A. Lidar, and Matthias Troyer. Defining and detecting quantum speedup. *Science*, 345(6195), 2014. 11

[10] Vasil S. Denchev, Sergio Boixo, Sergei V. Isakov, Nan Ding, Ryan Babbush, Vadim Smelyanskiy, John Martinis, and Hartmut Neven. What is the computational value of finite-range tunneling? *Phys. Rev. X*, 6:031015, Aug 2016. 11

[11] Daniel A. Lidar and Tood A. Brun, editors. *Quantum Error Correction*. Cambridge University Press, 2013. 11, 17, 39, 40, 41, 44, 45, 49, 58

[12] Ulrich Weiss. *Quantum Dissipative Systems*. World Scientific, 3 ed edition, 2008. 11, 41, 46

[13] Amir O. Caldeira. *An Introduction to Macroscopic Quantum Phenomena and Quantum Dissipation*. Cambridge University Press, 2014. 12, 38, 41, 45, 46

[14] H. P. Breuer and F. Petruccione. *The Theory of Open Quantum Systems*. Oxford University Press, Oxford, UK, 2002. 12, 38, 41, 42, 43

[15] E. Novais, E. R. Mucciolo, and H. U. Baranger. Resilent Quantum Computation in Correlated Environments: A Quantum Phase Transition Perspective. *Phys. Rev. Lett.*, 98:040501, 2007. 12, 41, 49

[16] E. Novais and Eduardo R. Mucciolo. Surface code threshold in the presence of correlated errors. *Phys. Rev. Lett.*, 110:010502, Jan 2013. 12, 51

[17] Pejman Jouzdani, E. Novais, I. S. Tupitsyn, and Eduardo R. Mucciolo. Fidelity threshold of the surface code beyond single-qubit error models. *Phys. Rev. A*, 90:042315, Oct 2014. 12, 51, 70

[18] Benjamin J. Brown, Daniel Loss, Jiannis K. Pachos, Chris N. Self, and James R. Wootton. Quantum Memories at Finite Temperature. *arXiv:1411.6643 [quant-ph]*, 2014. 16

[19] B Douçot and L B Ioffe. Physical implementation of protected qubits. *Rep. Prog. Phys.*, 75(072001), 2012. 16

[20] A. Yu. Kitaev. Fault-tolerant quantum computation by anyons. *Annals of Physics*, 303:2–30, 2003. 16

[21] W. K. Wootters and W. H. Zurek. A single quantum cannot be cloned. *Nature*, 299:802–803, 1982. 19

[22] Giuliano Benenti, Giulio Casati, and Guiliano Strini. *Principles of Quantum Computation and Information*, volume II. World Scientific, 1 edition, 2007. 22

[23] Dorit Aharonov. Quantum to classical phase transition in noisy quantum computers. *Phys. Rev. A*, 62:062311, Nov 2000. 27

[24] George B. Arfken and Hans J. Weber. *Mathematical Methods for Physicists*. Elsevier Academic Press, 2005. 29, 30, 87

[25] Sergey B. Bravyi and Alexei Yu. Kitaev. Quantum codes on a lattice with boundary. *arXiv:quant-ph/9811052v1*, 1998. 32

[26] Eric Dennis, Alexei Kitaev, Andrew Landahl, and John Preskill. Topological quantum memory. *J. Math. Phys.*, 43(9), 2002. 32, 35

[27] David S. Wang, Austin G. Fowler, and Lloyd C. L. Hollenberg. Surface code quantum computing with error rates over 1%. *Phys. Rev. A*, 83:020302, 2011. 32

[28] Austin G. Fowler, Matteo Mariantoni, John M. Martinis, and Andrew N. Cleland. Surface codes: Towards practical large-scale quantum computation. *Phys. Rev. A*, 86:032324, Sep 2012. 32

[29] James R. Wootton and Daniel Loss. High threshold error correction for the surface code. *Phys. Rev. Lett.*, 109:160503, Oct 2012. 32, 36

[30] R. Barends, J. Kelly, A. Megrant, A. Veitia, D. Sank, E. Jeffrey, T. C. White, J. Mutus, A. G. Fowler, B. Campbell, Y. Chen, Z. Chen, B. Chiaro, A. Dunsworth, C. Neill, P. O'Malley, P. Roushan, A. Vainsencher, J. Wenner, A. N. Korotkov, A. N. Cleland, and John M. Martinis. Superconducting quantum circuits at the surface code threshold for fault tolerance. *Nature*, 508:500–503, 24 April 2014. 33

[31] Charles D. Hill, Eldad Peretz, Samuel J. Hile, Matthew G. House, Martin Fuechsle, Sven Rogge, Michelle Y. Simmons, and Lloyd C. L. Hollenberg. A surface code quantum computer in silicon. *Science*, 2015. 33

[32] Masayuki Ohzeki. Error threshold estimates for surface code with loss of qubits. *Phys. Rev. A*, 85:060301, Jun 2012. 35

[33] H. Bombin, Ruben S. Andrist, Masayuki Ohzeki, Helmut G. Katzgraber, and M. A. Martin-Delgado. Strong resilience of topological codes to depolarization. *Phys. Rev. X*, 2:021004, Apr 2012. 35

[34] Thomas M. Stace and Sean D. Barrett. Error correction and degeneracy in surface codes suffering loss. *Phys. Rev. A*, 81:022317, 2010. 36

[35] A. O. Caldeira and A. J. Leggett. Quantum Tunnelling in a Dissipative System. *Annals of Physics*, 149:374–456, 1983. 37, 45

[36] A. J. Leggett and et. al. Dynamics of the dissipative two-state system. *Rev. of Mod. Phys.*, 59(1), 1987. 37, 46

[37] John H. Reina, Luis Quiroga, and Neil F. Johnson. Decoherence of quantum registers. *Physical Review A*, 65:032326, 2001. 45

[38] John Preskill. Sufficient condition on noise correlations for scalable quantum computing. *Quantum Information and Computation*, 13(34):181–194, 2012. 49

[39] E. Novais, Eduardo R. Mucciolo, and Harold U. Baranger. Hamiltonian formulation of quantum error correction and correlated noise: Effects of syndrome extraction in the long-time limit. *Phys. Rev. A*, 78:012314, 2008. 51

[40] Hui Khoon Ng and John Preskill. Fault-tolerant quantum computation versus gaussian noise. *Phys. Rev. A*, 79:032318, Mar 2009. 51

[41] P. Jouzdani, E. Novais, and E. R. Mucciolo. Fidelity of the surface code in the presence of a bosonic bath. *Phys. Rev. A*, 88:012336, Jul 2013. 51

[42] G. D. Mahan. *Many-Particle Physics*. Kluwer Academic/Plenum Publishers, 3 edition, 2000. 58

[43] J. Rammer and H. Smith. Quantum field-theoretical methods in transport theory of metals. *Rev. Mod. Phys.*, 58:323–359, Apr 1986. 58

[44] H. W. Capel. On the possibility of first-order phase transitions in Ising systems of triplet ions with zero-field splitting. *Physica*, 32:966–988, 1966. 69

[45] Lars Onsager. Crystal statistics. i. a two-dimensional model with an order-disorder transition. *Phys. Rev.*, 65:117–149, Feb 1944. 71

# Appendix A

# Fidelity

## A.1 Numerator $\langle\psi|\bar{\uparrow}\rangle\langle\bar{\uparrow}|\psi\rangle$

We start by working with the second factor of this product: $\langle\bar{\uparrow}|\psi\rangle$. To calculate this, we need to expand our evolved state $|\psi\rangle$ in terms of the alternating free evolutions $U(i)$ and syndrome extractions $\mathcal{P}_0$. For $N$ quantum error correction cycles, we have:

$$\langle\bar{\uparrow}|\psi\rangle = \langle\bar{\uparrow}|\mathcal{P}_0 U(N-1)\ldots\mathcal{P}_0 U(2)\,\mathcal{P}_0 U(1)\,\mathcal{P}_0 U(0)\,|\bar{\uparrow}\rangle|0\rangle \tag{A.1}$$

The next step is to substitute the explicit form of the projector and simplify. We know that the projection operator can be written as $\mathcal{P}_0 = |\bar{\uparrow}\rangle\langle\bar{\uparrow}| + \bar{X}|\bar{\uparrow}\rangle\langle\bar{\uparrow}|\bar{X}$, but we can write it in a more convenient way:

$$\mathcal{P}_0 = \sum_{\mathcal{J}} \mathcal{J}|\bar{\uparrow}\rangle\langle\bar{\uparrow}|\mathcal{J}, \tag{A.2}$$

where $\mathcal{J} = 1, \bar{X}$. Then we have:

$$\langle\bar{\uparrow}|\psi\rangle = \langle\bar{\uparrow}|\left(\sum_{\mathcal{J}}\mathcal{J}_N|\bar{\uparrow}\rangle\langle\bar{\uparrow}|\mathcal{J}_N\right)U(N-1)\ldots\left(\sum_{\mathcal{J}}\mathcal{J}_2|\bar{\uparrow}\rangle\langle\bar{\uparrow}|\mathcal{J}_2\right)U(1)\left(\sum_{\mathcal{J}}\mathcal{J}_1|\bar{\uparrow}\rangle\langle\bar{\uparrow}|\mathcal{J}_1\right)U(0)\,\mathcal{J}_0|\bar{\uparrow}\rangle|0\rangle \tag{A.3}$$

We label the $\mathcal{J}$ to keep track of terms through quantum error correction cycles, and we also we need to impose $\mathcal{J}_0 = I$. Now, since $\langle\bar{\uparrow}|\bar{X}|\bar{\uparrow}\rangle = 0$:

$$\langle\bar{\uparrow}|\left(\sum_{\mathcal{J}}\mathcal{J}_N|\bar{\uparrow}\rangle\langle\bar{\uparrow}|\mathcal{J}_N\right)U\left(N-1\right) = \langle\bar{\uparrow}|I|\bar{\uparrow}\rangle\langle\bar{\uparrow}|IU\left(N-1\right)$$
$$= \langle\bar{\uparrow}|U\left(N-1\right).$$

Also, if we constrain $\mathcal{J}_N = I$ we can rewrite this expression as:

$$\langle\bar{\uparrow}|\psi\rangle = \prod_{i=0}^{N-1}\sum_{\{\mathcal{J}\}}\langle\bar{\uparrow}|\mathcal{J}_{i+1}U\left(i\right)\mathcal{J}_i|\bar{\uparrow}\rangle|0\rangle$$

The other factor in the numerator is simply last equation's complex conjugate. The only extra detail is that we need to label differently the variables from the backwards evolution:

$$\langle\psi|\bar{\uparrow}\rangle = \sum_{\mathcal{KJ}}\langle 0|\prod_{i=N-1}^{0}\langle\bar{\uparrow}|\mathcal{K}_iU^{\dagger}\left(i\right)\mathcal{K}_{i+1}|\bar{\uparrow}\rangle$$

Putting these equations together, we get:

$$\langle\psi|\bar{\uparrow}\rangle\langle\bar{\uparrow}|\psi\rangle = \sum_{\mathcal{KJ}}\prod_{i=0}^{N-1}\langle 0|\langle\bar{\uparrow}|\mathcal{K}_iU^{\dagger}\left(i\right)\mathcal{K}_{i+1}|\bar{\uparrow}\rangle\prod_{j=N-1}^{0}\langle\bar{\uparrow}|\mathcal{J}_{j+1}U\left(j\right)\mathcal{J}_j|\bar{\uparrow}\rangle|0\rangle, \quad \text{(A.4)}$$

where we have the restrictions $\mathcal{K}_1 = \mathcal{K}_N = \mathcal{J}_0 = \mathcal{J}_N = I$ and $\sum_{\mathcal{KJ}} = \sum_{\mathcal{K}_1,\ldots\mathcal{K}_{N-1}}\sum_{\mathcal{J}_1\ldots\mathcal{J}_N}$.

## A.2 Denominator $\langle\psi|\psi\rangle$

As before, we expand $|\psi\rangle$ for $N$ quantum error correction cycles:

$$\langle\psi|\psi\rangle = \langle 0|\langle\bar{\uparrow}|U^{\dagger}\left(0\right)\mathcal{P}_0\ldots U^{\dagger}\left(N-1\right)\mathcal{P}_0U\left(N-1\right)\ldots\mathcal{P}_0U\left(0\right)|\bar{\uparrow}\rangle|0\rangle, \quad \text{(A.5)}$$

where we used the fact that $\mathcal{P}_0^2 = \mathcal{P}_0$. Now we use the explicit form of the projector and Equation (A.2).

$$\begin{aligned}\langle\psi|\psi\rangle &= \langle 0|\langle\bar{\uparrow}|U^{\dagger}(0)\left(\sum_{\mathcal{K}_1}\mathcal{K}_1|\bar{\uparrow}\rangle\langle\bar{\uparrow}|\mathcal{K}_1\right)\ldots U^{\dagger}(N-1)\left(\sum_{\mathcal{J}_N}\mathcal{J}_N|\bar{\uparrow}\rangle\langle\bar{\uparrow}|\mathcal{J}_N\right)U(N-1)\ldots \\ &\left(\sum_{\mathcal{J}_1}\mathcal{J}_1|\bar{\uparrow}\rangle\langle\bar{\uparrow}|\mathcal{J}_1\right)U(0)|\bar{\uparrow}\rangle|0\rangle\end{aligned} \tag{A.6}$$

To abbreviate this expression, we impose the restriction $\mathcal{J}_0 = \mathcal{K}_0 = I$. Also, just for the sake of notation, we write $\sum_{\mathcal{J}_N}\mathcal{J}_N|\bar{\uparrow}\rangle\langle\bar{\uparrow}|\mathcal{J}_N = \sum_{\mathcal{J}_N}\mathcal{K}_N|\bar{\uparrow}\rangle\langle\bar{\uparrow}|\mathcal{J}_N$, $\mathcal{K}_N = \mathcal{J}_N$. We get:

$$\begin{aligned}\langle\psi|\psi\rangle &= \langle 0|\langle\bar{\uparrow}|\mathcal{K}_0U^{\dagger}(0)\sum_{\mathcal{K}_1}\mathcal{K}_1|\bar{\uparrow}\rangle\langle\bar{\uparrow}|\mathcal{K}_1\ldots U^{\dagger}(N-1)\sum_{\mathcal{J}_N}\mathcal{K}_N|\bar{\uparrow}\rangle \\ &\langle\bar{\uparrow}|\mathcal{J}_NU(N-1)\ldots\sum_{\mathcal{J}_1}\mathcal{J}_1|\bar{\uparrow}\rangle\langle\bar{\uparrow}|\mathcal{J}_1U(0)\mathcal{J}_0|\bar{\uparrow}\rangle|0\rangle.\end{aligned} \tag{A.7}$$

In this way, we find an expression similar to the numerator's one, but with different restrictions:

$$\langle\psi|\psi\rangle = \sum_{\mathcal{KJ}}\langle 0|\prod_{i=0}^{N-1}\langle\bar{\uparrow}|\mathcal{K}_iU^{\dagger}(i)\mathcal{K}_{i+1}|\bar{\uparrow}\rangle\prod_{j=N-1}^{0}\langle\bar{\uparrow}|\mathcal{J}_{j+1}U(j)\mathcal{J}_j|\bar{\uparrow}\rangle|0\rangle, \tag{A.8}$$

where $\mathcal{J}_0 = \mathcal{K}_0 = I$, $\mathcal{K}_N = \mathcal{J}_N$, and $\sum_{\mathcal{KJ}} = \sum_{\mathcal{K}_1,\ldots\mathcal{K}_N}\sum_{\mathcal{J}_1\ldots\mathcal{J}_N}$.

## A.3 $\mathcal{A}$ and $\mathcal{B}$

We need to write the fidelity as a function of two quantities, $\mathcal{A}$ and $\mathcal{B}$:

$$\mathcal{F} = \frac{\langle\psi|\bar{\uparrow}\rangle\langle\bar{\uparrow}|\psi\rangle}{\langle\psi|\psi\rangle} = \frac{\mathcal{A}}{\mathcal{A}+\mathcal{B}}. \tag{A.9}$$

Then we know that:

$$\mathcal{B} = \langle\psi|\psi\rangle - \mathcal{A}. \tag{A.10}$$

We also know the expression for $\mathcal{A}$ (Appendix A.1), since it coincides with the numerator of the fidelity $\mathcal{A} = \langle\psi|\bar{\uparrow}\rangle\langle\bar{\uparrow}|\psi\rangle$.

We will now write it in terms of free evolution operators $U(i)$ and projection operators $\mathcal{P}_0$:

$$\mathcal{A} = \langle\bar{\uparrow}|U^{\dagger}(0)\,\mathcal{P}_0 \ldots U^{\dagger}(N-1)\,\mathcal{P}_0|\bar{\uparrow}\rangle\langle\bar{\uparrow}|\mathcal{P}_0 U(N-1)\ldots\mathcal{P}_0 U(0)\,|\bar{\uparrow}\rangle|0\rangle \tag{A.11}$$

Now we write the denominator of the fidelity and expand the projection operator $\mathcal{P}_0 = |\bar{\uparrow}\rangle\langle\bar{\uparrow}| + \bar{X}|\bar{\uparrow}\rangle\langle\bar{\uparrow}|\bar{X}$ at its center:

$$\begin{aligned}\langle\psi|\psi\rangle &= \langle 0|\langle\bar{\uparrow}|U^{\dagger}(0)\,\mathcal{P}_0 \ldots U^{\dagger}(N-1)\,\mathcal{P}_0 U(N-1)\ldots\mathcal{P}_0 U(0)\,|\bar{\uparrow}\rangle|0\rangle \\ &= \langle 0|\langle\bar{\uparrow}|U^{\dagger}(0)\,\mathcal{P}_0 \ldots U^{\dagger}(N-1)\left(|\bar{\uparrow}\rangle\langle\bar{\uparrow}| + \bar{X}|\bar{\uparrow}\rangle\langle\bar{\uparrow}|\bar{X}\right)U(N-1)\ldots\mathcal{P}_0 U(0)\,|\bar{\uparrow}\rangle|0\rangle\end{aligned} \tag{A.12}$$

Distributing the terms in the projection operator and identifying $\mathcal{A}$, from Equation (A.11), we get:

$$\langle\psi|\psi\rangle = \mathcal{A} + \langle 0|\langle\bar{\uparrow}|U^{\dagger}(0)\,\mathcal{P}_0 \ldots U^{\dagger}(N-1)\,\bar{X}|\bar{\uparrow}\rangle\langle\bar{\uparrow}|\bar{X}U(N-1)\ldots\mathcal{P}_0 U(0)\,|\bar{\uparrow}\rangle|0\rangle. \tag{A.13}$$

Comparing this last equation to Equation (A.10) we find the expression for $\mathcal{B}$, which can be abbreviated as:

$$\mathcal{B} = \sum_{\sigma,\tau}\sum_{\{\mathcal{K}\},\{\mathcal{J}\}}{}'' e^{-\mathcal{H}_1'}e^{-\mathcal{H}_2}\prod_{i=0}^{N-1}\langle\tau|\mathcal{K}_i\mathcal{K}_{i+1}G|\tau\rangle \times \prod_{i=N-1}^{0}\langle\sigma|\mathcal{J}_{i+1}\mathcal{J}_i G|\sigma\rangle, \tag{A.14}$$

where the sum $\sum''$ has the restrictions $\mathcal{J}_0 = \mathcal{K}_0 = I$, $\mathcal{J}_N = \mathcal{K}_N = \bar{X}$, and $\mathcal{J}_{i\neq 0,N} = \mathcal{K}_{i\neq 0,N} = \left\{I, \bar{X}\right\}$.

# Appendix B

# Green's Functions

We now want to compare the Green's functions involving auto-correlations with the ones that involve spatial and/or temporal correlations, ~~To this end,~~ so we evaluate our functions up to nearest neighbors. For the super-ohmic case, we will show that the ratio of Green's functions between nearest neighbors to Green's functions corresponding to auto-interaction goes to zero as the ultra-violet cutoff of the bath $\Lambda$ diverges.

Green's functions dealing with auto-correlations are the ones with $\mathbf{r} = \mathbf{r}'$ and $n = m$. When our functions involve spatial correlations we take $\mathbf{r} - \mathbf{r}' = \mathbf{a}$, where $\mathbf{a}$ is the lattice parameter. Finally, temporal correlations correspond to $n - m = 1$.

The Green functions with auto-correlations are:

$$\begin{aligned} F_c(0,0) &= \frac{\lambda^2 (v/\omega_0)^{D+2s}}{L^D} \sum_{\mathbf{k}\neq 0} |\mathbf{k}|^{2s} \cos(\mathbf{k}\cdot[\mathbf{r}-\mathbf{r}']) \cos([n-m]\,\omega_k\Delta) \frac{1-\cos(\omega_k\Delta)}{\omega_k^2} \\ &= \frac{\lambda^2 (v/\omega_0)^{D+2s}}{L^D} \sum_{\mathbf{k}\neq 0} |\mathbf{k}|^{2s} \frac{1-\cos(\omega_k\Delta)}{\omega_k^2} \end{aligned} \tag{B.1}$$

And for first-neighbors spatially and in time:

$$\begin{aligned} F_c(0,n-m=1) &= \frac{\lambda^2 (v/\omega_0)^{D+2s}}{L^D} \sum_{\mathbf{k}\neq 0} |\mathbf{k}|^{2s} \cos([n-m]\,\omega_k\Delta) \frac{1-\cos(\omega_k\Delta)}{\omega_k^2} \\ &= \frac{\lambda^2 (v/\omega_0)^{D+2s}}{L^D} \sum_{\mathbf{k}\neq 0} |\mathbf{k}|^{2s} \cos(\omega_k\Delta) \frac{1-\cos(\omega_k\Delta)}{\omega_k^2}, \end{aligned} \tag{B.2}$$

$$F_c\left(\mathbf{r}-\mathbf{r}',0\right) = \frac{\lambda^2\left(v/\omega_0\right)^{D+2s}}{L^D}\sum_{\mathbf{k}\neq 0}\left|\mathbf{k}\right|^{2s}\cos\left(\mathbf{k}\cdot\left[\mathbf{r}-\mathbf{r}'\right]\right)\cos\left(\left[n-m\right]\omega_k\Delta\right)\frac{1-\cos\left[\omega_k\Delta\right]}{\omega_k^2}$$
$$= \frac{\lambda^2\left(v/\omega_0\right)^{D+2s}}{L^D}\sum_{\mathbf{k}\neq 0}\left|\mathbf{k}\right|^{2s}\cos\left(\mathbf{k}\cdot\mathbf{a}\right)\frac{1-\cos\left[\omega_k\Delta\right]}{\omega_k^2}, \qquad \text{(B.3)}$$

$$F_c\left(\mathbf{r}-\mathbf{r}',n-m\right) = \frac{\lambda^2\left(v/\omega_0\right)^{D+2s}}{L^D}\sum_{\mathbf{k}\neq 0}\left|\mathbf{k}\right|^{2s}\cos\left(\mathbf{k}\cdot\left[\mathbf{r}-\mathbf{r}'\right]\right)\cos\left(\left[n-m\right]\omega_k\Delta\right)\frac{1-\cos\left[\omega_k\Delta\right]}{\omega_k^2}$$
$$= \frac{\lambda^2\left(v/\omega_0\right)^{D+2s}}{L^D}\sum_{\mathbf{k}\neq 0}\left|\mathbf{k}\right|^{2s}\cos\left(\mathbf{k}\cdot\mathbf{a}\right)\cos\left(\omega_k\Delta\right)\frac{1-\cos\left[\omega_k\Delta\right]}{\omega_k^2}, \qquad \text{(B.4)}$$

$$\Phi_{2,s}\left(\mathbf{r}-\mathbf{r}',n-m\right) = \frac{\lambda^2\left(v/\omega_0\right)^{D+2s}}{L^D}\sum_{\mathbf{k}\neq 0}\left|\mathbf{k}\right|^{2s}\sin\left(\mathbf{k}\cdot\left[\mathbf{r}-\mathbf{r}'\right]\right)\sin\left(\left[n-m\right]\omega_k\Delta\right)\frac{1-\cos\left[\omega_k\Delta\right]}{\omega_k^2}$$
$$= \frac{\lambda^2\left(v/\omega_0\right)^{D+2s}}{L^D}\sum_{\mathbf{k}\neq 0}\left|\mathbf{k}\right|^{2s}\sin\left(\mathbf{k}\cdot\mathbf{a}\right)\sin\left(\omega_k\Delta\right)\frac{1-\cos\left[\omega_k\Delta\right]}{\omega_k^2}, \qquad \text{(B.5)}$$

$$\Phi_1\left(\mathbf{r}-\mathbf{r}'\right) = \frac{\lambda^2\left(v/\omega_0\right)^{D+2s}}{L^D}\sum_{\mathbf{k}}\left|\mathbf{k}\right|^{2s}\cos\left[\mathbf{k}\cdot\left(\mathbf{r}-\mathbf{r}'\right)\right]\frac{\omega_k\Delta+\sin\left(\omega_k\Delta\right)}{\omega_k^2}$$
$$= \frac{\lambda^2\left(v/\omega_0\right)^{D+2s}}{L^D}\sum_{\mathbf{k}}\left|\mathbf{k}\right|^{2s}\cos\left(\mathbf{k}\cdot\mathbf{a}\right)\frac{\omega_k\Delta-\sin\left(\omega_k\Delta\right)}{\omega_k^2}. \qquad \text{(B.6)}$$

We will assume a dispersion relation:

$$\omega_{\mathbf{k}} = v\left|\mathbf{k}\right|, \qquad \text{(B.7)}$$

which is adequate for small energies.

We assume also a two-dimensional bath. Then in the continuum limit, $k\to\rho$, we have $\frac{(2\pi)^2}{L^2}\sum_{\mathbf{k}}\to\int_0^{\Lambda}\rho d\rho\int_0^{2\pi}d\theta$.

Let us start by writing expressions for $F_c\left(\mathbf{r}-\mathbf{r}',n-m\right)$, $\Phi_{2,s}\left(\mathbf{r}-\mathbf{r}',n-m\right)$, and $\Phi_1\left(\mathbf{r}-\mathbf{r}'\right)$:

$$\begin{aligned} F_c(\mathbf{a},1) &= \frac{\lambda^2 (v/\omega_0)^{2+2s}}{(2\pi)^2} \int_0^{\Lambda} \rho d\rho \int_0^{2\pi} d\theta \rho^{2s} \cos(\rho a \cos\theta) \cos(v\rho\Delta) \frac{1-\cos(v\rho\Delta)}{v^2\rho^2} \\ &= \frac{\lambda^2 (v/\omega_0)^{2+2s}}{(2\pi)^2 v^2} \int_0^{\Lambda} d\rho \rho^{2s-1} \cos(v\rho\Delta) [1-\cos(v\rho\Delta)] \int_0^{2\pi} d\theta \cos(\rho a \cos\theta) \end{aligned} \quad \text{(B.8)}$$

$$\begin{aligned} \Phi_{2,s}(\mathbf{a},1) &= \frac{\lambda^2 (v/\omega_0)^{2+2s}}{(2\pi)^2} \int_0^{\Lambda} \rho d\rho \int_0^{2\pi} d\theta \rho^{2s} \sin(\rho a \cos\theta) \sin(v\rho\Delta) \frac{1-\cos(v\rho\Delta)}{v^2\rho^2} \\ &= \frac{\lambda^2 (v/\omega_0)^{2+2s}}{(2\pi)^2 v^2} \int_0^{\Lambda} d\rho \rho^{2s-1} \sin(v\rho\Delta) [1-\cos(v\rho\Delta)] \int_0^{2\pi} d\theta \sin(\rho a \cos\theta) \end{aligned} \quad \text{(B.9)}$$

$$\Phi_1(\mathbf{a}) = \frac{\lambda^2 (v/\omega_0)^{2+2s}}{(2\pi)^2 v^2} \int_0^{\Lambda} d\rho \rho^{2s-1} [v\rho\Delta - \sin(v\rho\Delta)] \times \int_0^{2\pi} d\theta \cos(\rho a \cos\theta) \quad \text{(B.10)}$$

Now we change to the variables:

$$x = v\Delta\rho \implies \rho = \frac{x}{v\Delta} \quad \text{(B.11)}$$

$$d\rho = \frac{dx}{v\Delta} \quad \text{(B.12)}$$

$$z = \frac{|\mathbf{a}|}{v\Delta} \implies a = v\Delta z \quad \text{(B.13)}$$

Then we get:

$$\begin{aligned} F_c(\mathbf{a},1) &= \frac{\lambda^2 (v/\omega_0)^{2+2s}}{(2\pi)^2 v^2} \int_0^{v\Delta\Lambda} \frac{dx}{v\Delta} \left(\frac{x}{v\Delta}\right)^{2s-1} \cos x (1-\cos x) \int_0^{2\pi} d\theta \cos\left(\frac{x}{v\Delta} v\Delta z \cos\theta\right) \\ &= \frac{\lambda^2 (v/\omega_0)^{2+2s}}{(2\pi)^2 v^{2s+2} \Delta^{2s}} \int_0^{v\Delta\Lambda} dx \cdot x^{2s-1} \cos x (1-\cos x) \int_0^{2\pi} d\theta \cos(xz\cos\theta) \end{aligned} \quad \text{(B.14)}$$

$$\Phi_{2,s}(z,1) = \frac{\lambda^2 (v/\omega_0)^{2+2s}}{(2\pi)^2 v^{2s+2} \Delta^{2s}} \int_0^{v\Delta\Lambda} dx \cdot x^{2s-1} \sin x (1-\cos x) \int_0^{2\pi} d\theta \sin(xz\cos\theta) \quad \text{(B.15)}$$

$$\Phi_1(z) = \frac{\lambda^2 (v/\omega_0)^{2+2s}}{(2\pi)^2 v^{2s+2}\Delta^{2s}} \int_0^{v\Delta\Lambda} dx \cdot x^{2s-1}(x - \sin x) \int_0^{2\pi} d\theta \cos(xz\cos\theta) \tag{B.16}$$

The angular part can be expressed as a Bessel function[1]:

$$\int_0^{2\pi} d\theta \cos(xz\cos\theta) = 2\pi J_0(xz) \tag{B.17}$$

On the other hand, $\Phi_{2,s}$'s angular integral is

$$\int_0^{2\pi} d\theta \sin(xz\cos\theta) = 0 \tag{B.18}$$

So:

$$F_c(\mathbf{a}, 1) = \frac{\lambda^2 (v/\omega_0)^{2+2s}}{2\pi v^{2s+2}\Delta^{2s}} \int_0^{v\Delta\Lambda} dx \cdot x^{2s-1} \cos x (1 - \cos x) J_0(xz) \tag{B.19}$$

$$\Phi_{2,s}(z, 1) = 0 \tag{B.20}$$

$$\Phi_1(z) = \frac{\lambda^2 (v/\omega_0)^{2+2s}}{2\pi v^{2s+2}\Delta^{2s}} \int_0^{v\Delta\Lambda} dx \cdot x^{2s-1}(x - \sin x) J_0(xz) \tag{B.21}$$

The ohmic case is defined by the logarithmic divergence:

$$2s - 1 = -1, \tag{B.22}$$

so that $s = 0$ corresponds to the ohmic case, $s > 0$ is super-ohmic, and $s < 0$ is sub-ohmic.

Let us now evaluate the super-ohmic case.

## $2s - 1 = 0$ **or** $s = 1/2$.

We need to evaluate: $F_c(0, 0)$, $F(0, 1)$, $F_c(\mathbf{r} - \mathbf{r}', 0)$, $F_c(\mathbf{r} - \mathbf{r}', n - m)$, and $\Phi_1(\mathbf{r} - \mathbf{r}')$.

We have $s = \frac{1}{2} \implies 2s - 1 = 0 \implies 2s = 1$, and $2s + 2 = 3$.

[1] Equation 11.30, [24]

$$\begin{aligned} F_c(0,0) &= \frac{\lambda^2 (v/\omega_0)^3}{2\pi v^3 \Delta} \int_0^{v\Delta\Lambda} dx\,(1-\cos x) \\ &\approx \frac{\lambda^2 v}{2\pi\omega_0^3}\Lambda \end{aligned} \tag{B.23}$$

$$\begin{aligned} F_c(z=0,1) &= \frac{\lambda^2 (v/\omega_0)^3}{2\pi v^3 \Delta} \int_0^{v\Delta\Lambda} dx \cos x\,(1-\cos x) \\ &= \frac{\lambda^2 (v/\omega_0)^3}{2\pi v^3 \Delta} \left[\sin(v\Delta\Lambda) - \frac{v\Delta\Lambda + \sin(2v\Delta\Lambda)}{2}\right] \\ &\approx -\frac{\lambda^2 v}{2\pi\omega_0^3}\frac{\Lambda}{2} \end{aligned} \tag{B.24}$$

$$\begin{aligned} F_c\left(z=\frac{a}{v\Delta},0\right) &= \frac{\lambda^2 (v/\omega_0)^3}{2\pi v^3 \Delta} \int_0^{v\Delta\Lambda} dx \cdot (1-\cos x)\, J_0\left(\frac{xa}{v\Delta}\right) \\ &= \frac{\lambda^2}{2\pi\omega_0^3\Delta} \int_0^{v\Delta\Lambda} dx \cdot \left[J_0\left(\frac{xa}{v\Delta}\right) - \cos x \cdot J_0\left(\frac{xa}{v\Delta}\right)\right] \end{aligned} \tag{B.25}$$

Here the relevant integrals are:

$$\int_0^\infty dx J_0(zx) = \frac{1}{z} \tag{B.26}$$

and

$$\int_0^\infty dx \cos x \cdot J_0(zx) = \begin{cases} \frac{1}{\sqrt{z^2-1}}, & 1 < z \\ \infty, & z = 1 \\ 0, & 0 < z < 1 \end{cases} \tag{B.27}$$

Then, for $z > 1$,

$$F_c\left(z=\frac{a}{v\Delta},0\right) = \frac{\lambda^2 (v/\omega_0)^3}{2\pi v^3\Delta}\left(\frac{1}{z} + \frac{1}{\sqrt{z^2-1}}\right)$$

$$F_c\left(z=\frac{a}{v\Delta},1\right) = \frac{\lambda^2\left(v/\omega_0\right)^3}{2\pi v^3\Delta}\int_0^{v\Delta\Lambda} dx\cdot\cos x\left(1-\cos x\right)J_0\left(\frac{xa}{v\Delta}\right)$$
$$= \frac{\lambda^2}{2\pi\omega_0^3\Delta}\int_0^{v\Delta\Lambda} dx\left[\cos x\cdot J_0\left(\frac{xa}{v\Delta}\right)-\cos^2 x\cdot J_0\left(\frac{xa}{v\Delta}\right)\right] \quad \text{(B.28)}$$

Now the relevant integrals are B.27, and:

$$\int_0^\infty dx\cos^2 x\cdot J_0\left(xz\right) = \begin{cases}\frac{1}{2z}+\frac{1}{2\sqrt{z^2-4}}, & 2<z\\ \frac{1}{2z}, & 0<z<2\end{cases} \quad \text{(B.29)}$$

Now for $z>2$:

$$F_c\left(z=\frac{a}{v\Delta},1\right) = \frac{\lambda^2}{2\pi v^3\Delta}\left(\frac{1}{\sqrt{z^2-1}}-\frac{1}{2z}-\frac{1}{2\sqrt{z^2-4}}\right) \quad \text{(B.30)}$$

$$\Phi_1\left(z=\frac{a}{v\Delta}\right) = \frac{\lambda^2}{2\pi v^3\Delta}\int_0^{v\Delta\Lambda} dx\cdot\left(x-\sin x\right)J_0\left(\frac{xa}{v\Delta}\right)$$
$$= \frac{\lambda^2}{2\pi v^3\Delta}\int_0^{v\Delta\Lambda} dx\cdot\left[xJ_0\left(\frac{xa}{v\Delta}\right)-\sin x\cdot J_0\left(\frac{xa}{v\Delta}\right)\right] \quad \text{(B.31)}$$

Now the relevant integrals are:

$$\int_0^{v\Delta\Lambda} dx\cdot xJ_0\left(zx\right) = xJ_1\left(x\right)\Big|_0^{v\Delta\Lambda}\approx v\Delta\Lambda\sqrt{\frac{2}{\pi v\Delta\Lambda}}$$
$$= \sqrt{\frac{2}{\pi}v\Delta\Lambda} \quad \text{(B.32)}$$

and

$$\int_0^\infty dx\sin x J_0\left(zx\right) = \begin{cases}0, & 1<z\\ \frac{1}{\sqrt{1-z^2}}, & 0<z<1\end{cases} \quad \text{(B.33)}$$

For $z>1$:

$$\Phi_1\left(z=\frac{a}{v\Delta}\right)\approx\frac{\lambda^2\left(v/\omega_0\right)^3}{2\pi v^3\Delta}\sqrt{\frac{2}{\pi}v\Delta\Lambda}\approx\frac{\lambda^2\left(v/\omega_0\right)^3}{\sqrt{2\pi^3v^5\Delta}}\Lambda^{1/2} \quad \text{(B.34)}$$

Putting everything together:

$$\frac{F_c(z,0)}{F_c(0,0)} \sim \frac{F_c(z,1)}{F_c(0,0)} \sim \frac{F_c(z,0)}{F_c(0,1)} \sim \frac{F_c(z,1)}{F_c(0,1)} \sim \frac{1}{\Lambda} \tag{B.35}$$

and

$$\frac{\Phi_1(z)}{F_c(0,0)} \sim \frac{\Phi_1(z)}{F_c(0,1)} \sim \frac{1}{\Lambda^{1/2}}. \tag{B.36}$$